Stratigraphy of deformed Permian carbonate reefs in the Saraburi Province, Thailand

Thesis submitted in accordance with the requirements of the University of Adelaide for an Honours Degree in Geology

Romana Elysium Carthew Dew

November 2014

THE UNIVERSITY of ADELAIDE

TITLE

Stratigraphy of deformed Permian carbonate reefs in the Saraburi Province, Thailand

RUNNING TITLE

Stratigraphy of deformed Permian carbonate reefs, Thailand

ABSTRACT

The Indosinian Orogeny brought together a number of continental blocks and volcanic arcs during the Permian and Triassic periods. Prior to the orogeny, carbonate platforms and minor clastic sediments were deposited on the margins of these continental blocks. The Khao Khwang Platform formed along the southern margin of one continental fragment of the Indochina Block and was deformed in the early Triassic creating the Khao Khwang Fold-Thrust Belt.

The palaeogeography of the Indochina Block margin prior to this deformation is incompletely known, yet is significant in assisting with structural reconstructions of the area and in assisting with our understanding of the ecology of Permian fusulinid-dominated habitats. The sedimentology and stratigraphy of the Permian platform carbonates and basin complexes require further analysis. Three main carbonate platform dominated facies have been identified previously as the Phu Phe, Khao Khad and Khao Khwang formations. These platform facies are divided by clastic, mixed siliciclastic and carbonate sequences known as the Sap Bon, Pang Asok and Nong Pong formations.

Here, I present a stratigraphic model for the carbonate reefs and intervening clastic sedimentary rocks using the exposed well-developed sections in central Thailand. The model integrates fossil identification, biostratigraphic correlation and palaeoenvironmental analysis, in accordance with structural controls and fieldwork in the Saraburi Province, Thailand. Eleven sections were logged, encompassing units from three thrust sheets. The stratigraphic logs suggest five depositional environments for the middle Permian sequences, dated using foraminifera and algae. Characteristics of mass transport were identified indicating basinal facies receiving turbid debris flows. Furthermore, depositional texture variations indicated energy changes from peritidal, lagoonal through to reef environments. The palaeoenvironmental inferences and fossil identification allow section correlation and assist in unravelling the structure of this fold-thrust belt.

KEYWORDS

Permian biostratigraphy, carbonate stratigraphy, Khao Khwang Fold-Thrust Belt, Khao Khad Formation, carbonate platform, fusulinid.

TABLE OF CONTENTS

LIST OF FIGURES

INTRODUCTION

The Khao Khwang Platform is a late Pennsylvanian to Permian carbonate and mixed clastic sequence located in central Thailand (Figure 1). It formed as an elongate carbonate platform along the edge of the Indochina Block (Ueno and Charoentitirat 2011). The Khao Khwang Platform is interpreted to have formed in similar conditions to present-day carbonate platforms in clear, shallow, tropical waters of moderate salinity and little siliciclastic input (Bunopas 1992, Ueno and Charoentitirat 2011). The study area is located primarily within the Khao Khad Formation, an 1800 m thick intercalated carbonate and clastic sequence of the Saraburi Group, which crops out in a WNW to ESE trending belt in the Saraburi Province (Figure 1, Ueno and Charoentitirat 2011).

The Khao Khwang Platform was deformed during the Indosinian Orogeny, between the latest Permian and Lower Triassic, resulting in the Khao Khwang Fold-Thrust Belt (Helmcke 1985, Sone and Metcalfe 2008, Morley et al. 2013). The Permo-Triassic Phra Ngam Diorite and Khao Yai Volcanics were extruded into and intruded within the Saraburi Group coeval with deposition (Chutakositkanon et al. 2000, Ueno et al. 2012).

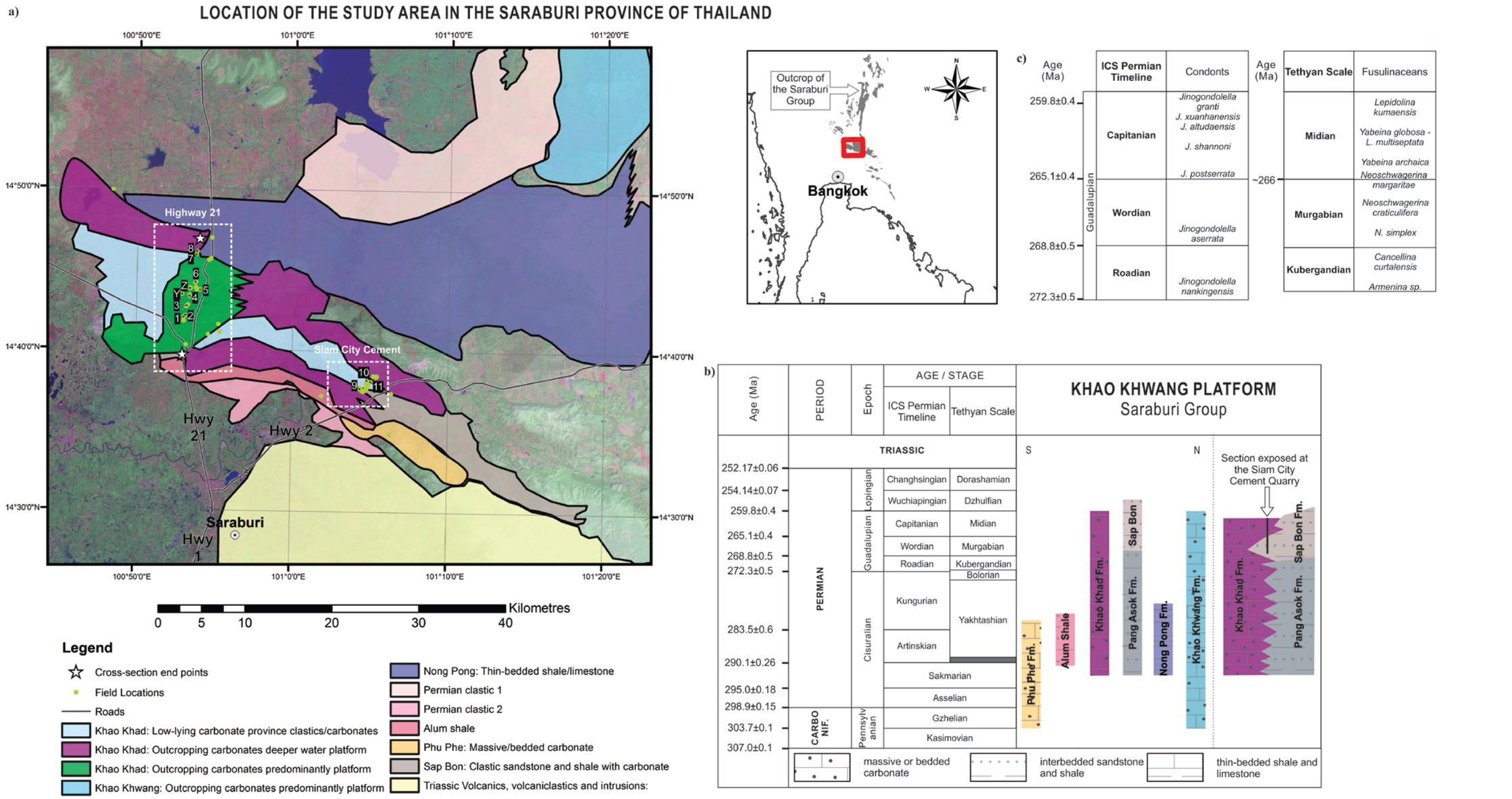

Figure 1: a) Location map portraying the regional stratigraphy, cross-section and field locations b) Stratigraphic log of the Khao Khwang Platform in the Saraburi Province c) Comparisons between the International Permian Timeline and the Tethyan Scale, dates are determined by the first appearance datum (FAD) of fossils highlighted; modified from Menning et al. (2006) Ueno and Charoentitirat (2011), Morley et al. (2013) and Shen et al. (2013)

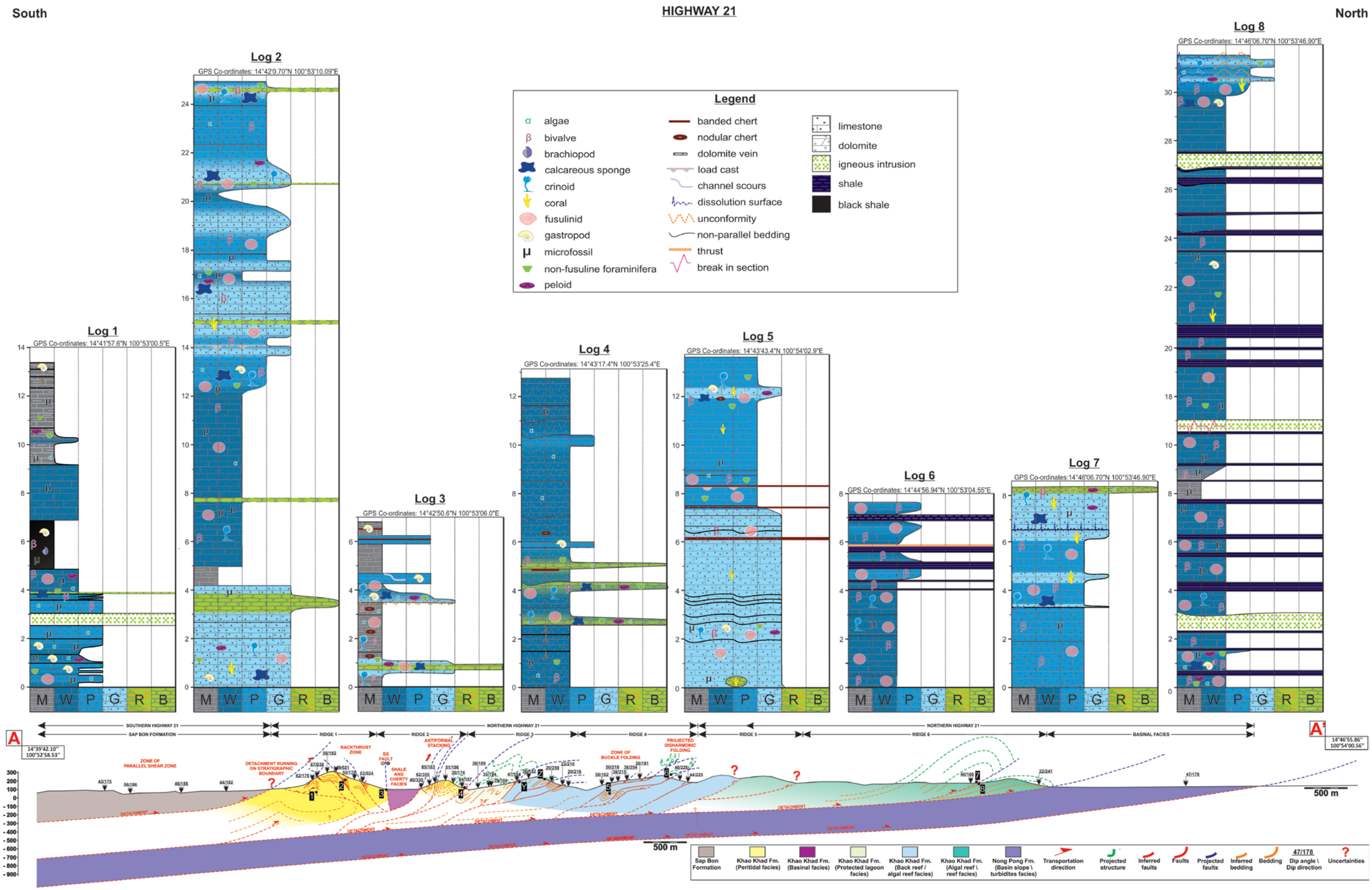

Figure 2: Regional cross-section through the southern portion of the Saraburi Region, the Khao Khwang Fold-Thrust Belt with stratigraphic sections superimposed scale in metres, M=Mudstone, W=Wackestone, P=Packstone, G=Grainstone, R=Rudstone, B=Boundstone (modified Arboit et al. (in press))

The Khao Khwang Platform contains diverse algae and foraminifera, which have been studied taxonomically (Dawson and Racey 1993, Udchachon et al. 2014). Previous sedimentological and stratigraphic studies, however, did not recognise the recently described structural complexity (e.g. Chutakositkanon et al. 2000, Thambunya et al. 2007). Many of the stratigraphic units have been named informally without thorough definitions and descriptions; without comprehensive regional work completed on detailed lithology, depositional environments and diagenetic history (Thambunya et al. 2007, Ueno and Charoentitirat 2011). Furthermore, many stratigraphic works have failed to incorporate the available palaeontological data (Ueno and Charoentitirat 2011). Moreover, Dawson & Racey (1993) is the only study to introduce the possibility of structural complications into their stratigraphic analysis of the Highway 21. Within the last 21 years, the structure of the region has been refined and recent studies have shown that low angle kilometre-scale thrusts deform the stratigraphy (Morley et al. 2013, Arboit et al. in press). Therefore, this study aims to redescribe the sedimentology and interpret the shallow marine depositional environments of the Khao Khad Formation in light of the newly described structural cross-sections published through the region (Arboit et al. in press).

In this paper, I attempt to reconstruct the original distribution of the facies by using the structural balancing presented in Arboit et al. (in press) and from this interpret the palaeogeography and palaeoecology of the platform. In this study, I demonstrate that the Khao Khad Formation formed in a shallow marine carbonate platform setting, using a series of stratigraphic logs from 11 field locations along Highway 21 and from the Siam City Cement Quarry along Highway 2 (Figure 1). I then use macrofacies and

microfacies analysis to create biostratigraphic correlations and facies associations to reconstruct a model for the depositional setting of the Khao Khad Formation.

CARBONATES AND THEIR DEPOSITIONAL ENVIRONMENTS

Carbonates constitute 20-25% of all sedimentary rocks in the global geologic record and are host to about half of the world's major petroleum reservoirs (James 1977, Tucker 2001, Boggs 2011b). Permian carbonates are prolific throughout Thailand and are economically significant for cement and stone production (Thambunya et al. 2007). The carbonate mineral identification is advantageous for economic and palaeoenvironmental applications. Of the sixty carbonate minerals, three are significant for environmental interpretation: calcite, aragonite and dolomite (Boggs 2011b). Ultimately, all aragonite and magnesian calcite marine cements stabilise to calcite and dolomite through dissolution and reprecipitation processes (MacKenzie and Adams 2007, Moore and Wade 2013). The stabilisation process results in a loss of the original geochemical information and textural details, which becomes problematic for recognising ancient marine cements, especially in the aragonite seas of the upper Paleozoic, Paleogene and Neogene (Wright and Burchette 1996, Moore and Wade 2013). Dolomite is predominantly a secondary product of calcite or aragonite transformation, especially prevalent with reef limestones. Although dolomite does occur as a primary mineral in magnesium enriched seawaters and in association with sulphide ore hydrothermal vein systems (Tucker and Wright 1990, Luhr 2003, MacKenzie and Adams 2007). Mineral replacement can occur early in diagenesis, soon after deposition, prior to compaction or later in the burial process (Tucker 2001, MacKenzie and Adams 2007)

Modern carbonate platforms are often insightful analogues for ancient carbonate environments. Most modern carbonate production occurs in clear, shallow, warm waters of moderate salinity and little siliciclastic input between latitudes of 30°N and 30°S (James 1977, Wright and Burchette 1996, Boggs 2011a). Modern and ancient carbonate platforms occur in six depositional settings (Figure 3) and the type of carbonate platform that develops depends on tectonics and relative sea level change (Tucker and Wright 1990, Wright and Burchette 1998, Tucker 2001, Flügel 2010). The type and amount of carbonate production is influenced partly by the type of carbonate platform, with shallow marine tropical reefs producing the most carbonates (Wright and Burchette 1996, Luhr 2003).

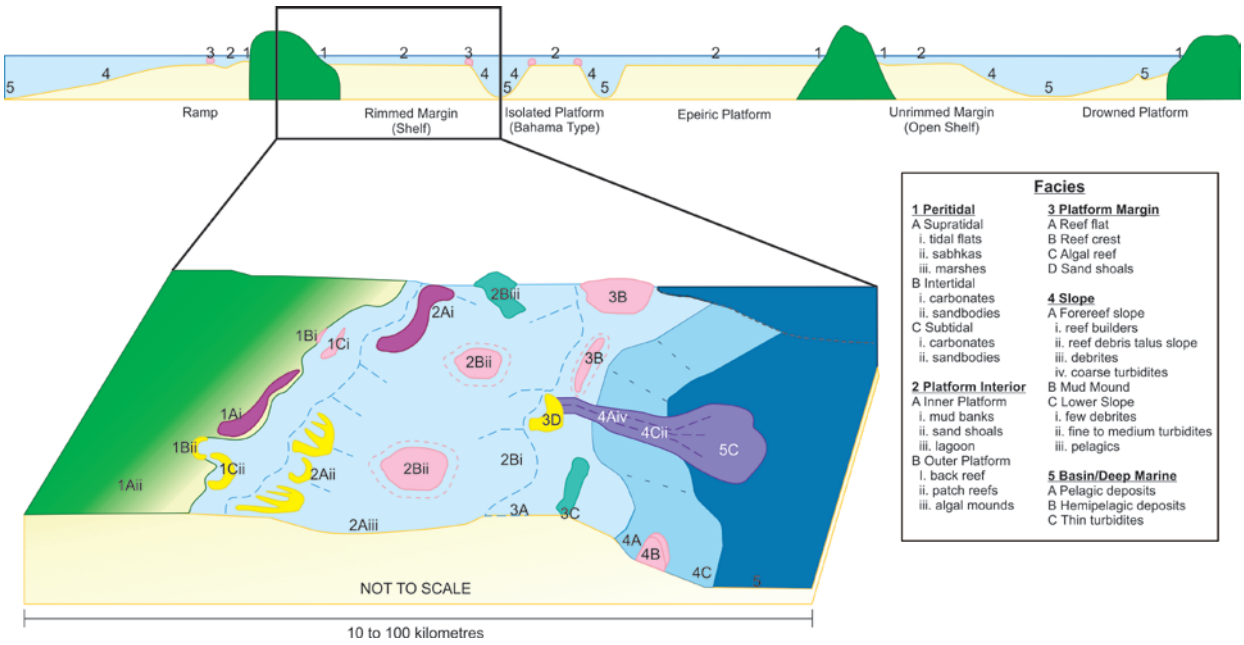

Figure 3: Diagram depicting the characteristics of the six depositional settings of carbonate platforms incorporating information from Wright and Burchette (1996), Wright and Burchette (1998), Chutakositkanon et al. (2000), Tucker (2001), Flügel (2010) and Boggs (2011a).

PERMIAN REEF DEVELOPMENT

The Permian is a time of major reef building as seen throughout Thailand (Weidlich 2002, Kiessling et al. 2003, Udchachon et al. 2014). Reefs at this time have been

divided into three compositional types: microbial reefs, metazoan reefs and calcareous algae reefs (Weidlich 2002). Crinoids and siliceous sponges increased during the Permian indicating a cooling trend from the earlier warmer waters that were conducive to deposition of peloids and aragonitic shells and cements (Kiessling et al. 2003). The climax of Permian reef growth occurred in the Guadalupian Epoch with high reef diversity with all three reef compositional types in addition to the extent, abundance and size of reef localities (Weidlich 2002). At the end of the Guadalupian, a combination of decreasing global sea level, regional salinity fluctuations and micro-continent collision led to a loss of >89% carbonate production (Weidlich 2002, Udchachon et al. 2014). The end-Guadalupian crisis terminated the reef domain of the Indochina Platform (Weidlich 2002). This is indicated in the fossil record with the abrupt decline in large fusulinids, a type of tropical benthic foraminifera, which were major reef builders during the Guadalupian (BouDagher-Fadel 2008, Davydov 2013, Hada et al. in press).

KHAO KHWANG FOLD-THRUST BELT

The carbonate platforms associated with the Khao Khwang Fold-Thrust Belt are situated extensively along the edge of the Indochina Block, on the eastern side of the Chao Phraya central plain and western margin of Khorat Plateau (Chutakositkanon et al. 2000, Ueno and Charoentitirat 2011, Ueno et al. 2012).

In the Saraburi region, the carbonates of the Khao Khwang Platform were deposited between the Upper Pennsylvanian and the late Permian (Ueno and Charoentitirat 2011). These sequences were once considered part of the Ratburi Limestone (Brown et al. 1951, Toriyama and Kanmera 1979, Dawson and Racey 1993) although subsequently they have been separated into the Saraburi Group due to the distinct faunal assemblages

present (Bunopas 1992). Paleozoic palaeomagnetic data indicate that the Saraburi Group was deposited at a palaeolatitude of nearly 10º south of the Permian equator (El Tabakh and Utha-Aroon 1998, Thambunya et al. 2007, Metcalfe 2013). Hinthong et al. (1985) identified three main formations that represented the facies in the carbonate platform. These are the Phu Phe, Khao Khad and Khao Khwang formations. These platform facies are divided by clastic, mixed siliciclastic and carbonate sequences, known as the Sap Bon, Pang Asok and Nong Pong formations (Chutakositkanon et al. 2000, Chonglakmani 2001). Although traditionally interpreted as a vertical stratigraphic succession, recent fossil data demonstrate that the carbonate sequences are mostly contemporaneous (Ueno and Charoentitirat 2011). Marine deposition of the Saraburi Group was terminated by uplift and deformation caused by the Indosinian Orogeny, sometime between the latest Permian and Ladinian (Baird and Bosence 1993, Sone and Metcalfe 2008).

KHAO KHAD FORMATION

The Khao Khad Formation of the Saraburi Group has been previously dated as middle Guadalupian and on the Tethyan Scale, predominantly Murgabian with limited extension into the Midian (Figure 1, Baird and Bosence 1993, Dawson and Racey 1993, Ueno and Charoentitirat 2011). The Tethyan Scale is zoned using fusulinids, in contrast to the conodonts being the primary fossil used for the biostratigraphic correlation for The International Commission on Stratigraphy (ICS) Permian Timeline (Figure 1, Wardlaw et al. 2004, Shen et al. 2013). Conodonts are insufficiently studied in the Tethys, hence fusulinids and to a lesser extent ammonoids are used to subdivide the Permian (Wardlaw et al. 2004). Although the ICS and Tethyan scales are broadly equivalent, as shown in Figure 1, the use of different determinants leads to differences

in the exact ages (Menning et al. 2006, Dickins et al. 2007, Henderson et al. 2012). For example, the Murgabian rocks are only provisionally correlated to the ICS Wordian as they lack the conodonts to establish a strong correlation (Menning et al. 2006).

The fusulinid-brachiopod-gastropod assemblages and overall bioclastic lithology imply that the Khao Khad Formation was deposited in a tropical shallow marine carbonate platform environment (Thambunya et al. 2007, Ueno and Charoentitirat 2011). The facies indicate that there was a transgressive and regressive cycle during the Cisuralian and Guadalupian (Dawson and Racey 1993, Chutakositkanon et al. 2000). These cycles are visible through changes in the lithological and palaeontological characteristics.

Further subdivisions of the Khao Khad Formation have been previously identified through fossil analysis using the abundance and diversity of fusuline and calcareous algal biota. Chutakositkanon et al. (2000) regroup the Khao Khad Formation in the Khao Pun area into two lithostratigraphic units, the Khao Sung and Khao Pun Formations that are subdivided into six members. In contrast, Thambunya et al. (2007) distinguished fifteen rock units of the Khao Khad Formation within their three study areas. Thambunya et al. (2007) also created a depositional model that infers the Khao Khad Formation formed from an inner shelf lagoon with a barrier bar/shallow platform in the outer shelf and foreslope. Dawson and Racey (1993) recognise six main biofacies in their study locations just north of Saraburi. It is also suggested that there was a sedimentary hiatus related to a worldwide marine regression in the early middle Permian, which caused a period of intense dolomitisation in carbonates of the Khao Khad Formation (Dawson and Racey 1993).

FIELD AND THIN SECTION ANALYSES

Fieldwork was carried out along Highway 21 and in Siam City Cement Quarry in the Saraburi Province of Thailand, approximately 100 kilometres NNE of Bangkok. The Saraburi Province was chosen due to the exceptionally exposed sections of the Permian carbonate reefs and intervening clastic sediments within the region. It is also an area of ongoing structural work and a better understanding of the area's stratigraphy will assist in unravelling the structure of the area.

Stratigraphic logs were constructed along with fossil identification, sketches, photographs and samples taken from the Saraburi Province. The sequences were classified using both the Dunham (1962) and Folk (1962) classification schemes. In total, stratigraphic logs were taken from 11 field locations to form the basis of facies interpretations and biostratigraphic correlation. Sections were numbered from south to north in Highway 21: Logs 1 to 8 and Logs 9 to 11 from Siam City Cement. The logs were digitised using CorelDRAW software (Figure 2).

Thirty-two samples were prepared into thin sections for optical microscopy. All 32 sections were then stained with Alizarin Red and potassium ferricyanide to discriminate calcite and dolomite as per Appendix A. The sections were then analysed under transmitted light to validate and add to the field interpretations as per Appendix A.

The fossil assemblages determined in the field and by thin section analysis were used to infer facies and their associations in addition to the age and timing of the sequences.

The facies and their associations were then used to reconstruct a model for the depositional setting of the Khao Khad Formation during the Permian.

FOSSILS AND LITHOLOGY OF THE KHAO KHAD FORMATION

Fossils from thin section analyses

FORAMINIFERA

Generally, the sequences are highly bioclastic, dominated by a variety of foraminifera. Five groups of fusulinids commonly appear in the thin section and are identified in Figure 4. *Verbeekinidae* are ~1 mm-500 µm in size with dark brown to black test walls and usually light coloured chambers. They are present in the Murgabian assemblage in Log 2 (Figure 2). *Neoschwagerinidae* have thick walls that are coated or encrusted with algae. Many of the larger foraminifera including the *Neoschwagerinidae* have a symbiotic relationship with photosynthetic algae that is indicated by this dark algal coating (Dawson and Racey 1993, Beavington-Penney and Racey 2004). This relationship is suggested to have evolved during the Carboniferous (Beavington-Penney and Racey 2004). *Neoschwagerinidae* are the largest fusulinids, generally increasing in diameter through the Permian. They appear in Log 8 (Figure 2) including the *Neoschwagerina* and *Gifuella sp.* of the middle and late Murgabian. The *Schwagerinidae* are few mm in diameter with strong contrast between the light storm grey of the test walls and the lighter colour of the chamber interiors (see Figure 4).

Schubertellidae are small elongate elliptical fusulinids with dark walls and usually light coloured chambers. They are present in Logs 1 and 2. *Staffellidae* are small elongate elliptical fusulinids that occur within well-agitated marine shoals. They appear taupe in

colour in thin section, lighter than other fusulinid groups. *Nankinella,* a member of this taxa, occur from the Sakmarian to Changhsingian. *Staffellidae* occur in the back reef of Logs 5 and 8 (Figure 2).

Four groups of non-fusuline foraminifera assisted in determining the age of samples (Figure 4). The "rose" group are distinguished as 500-200 µm rosebud shaped non-fusuline foraminifera. They are smaller than many of the more advanced fusulinids and include *Miliolida, Baisalina* and *Hemigordius sp.* This group of non-fusuline foraminifera are prolific throughout Logs 3 and 4 (Figure 2). The *Globivalvulina* group (Figure 4) is characterised by ~200 µm-sized foraminifera that have several chambers that link together to give the appearance of popped corn. Species of *Globivalvulina* are present in the global fossil record between 336.0 to 251.3 Ma. *Globivalvulina* sp. proliferate Log 4 (Figure 2). Other foraminifera are present in the samples but did not occur frequently and were less useful for constraining the age of the sequence, for example, the *Textulariidae* Group that have two columns of chambers that merge into one and still occur today. The ages for sections (1 and 4) that predominantly contain non-fusuline foraminifera were harder to constrain as their morphology changes occur at a slower rate than the rapidly evolving Permian fusulinids.

Varying degrees of preservation are present in the study area affecting the taxonomic identification of the fossils. The fusulinids in Log 5 and 9 (Figure 2) are generally less well preserved and subsequently fossils are harder to identify. Crosscutting veins and compaction are visible in some of the thin sections, particularly for Logs 7 and 10.

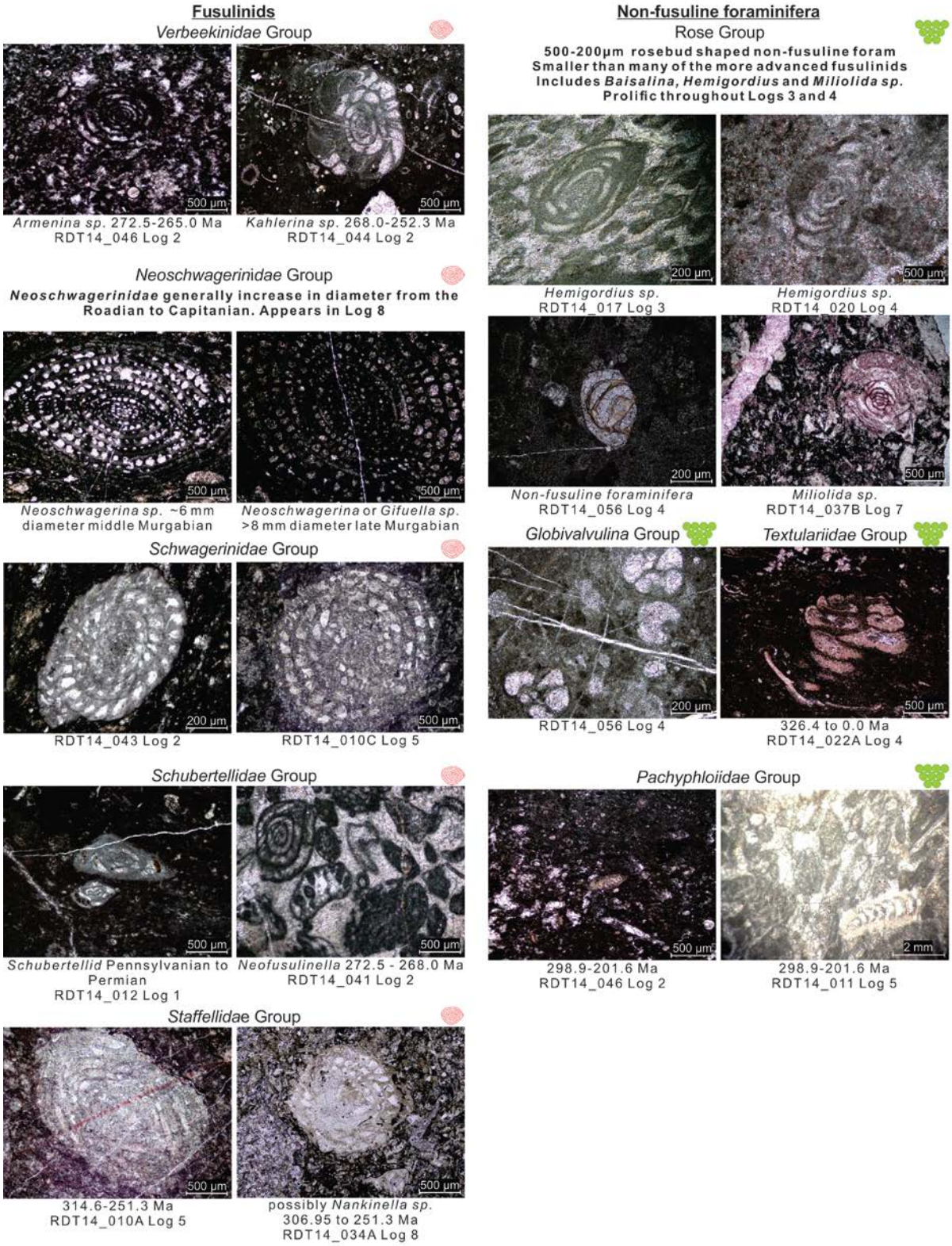

Figure 4: Distinct foraminiferal groups used to determine age distinguishing the fusulinid and non-fusuline foraminifera that are also distinguished in the stratigraphic sections of Figures 2 and 7. Information from Plummer (1948), Loeblich and Tappan (1964), Sartorio and Venturini (1988), Dawson & Racey (1993), Ueno and Sakagami (1993), BouDagher-Fadel (2008), Flügel (2010) and Kobayashi et al. (2010).

ALGAE

Four algal types: *Tubiphytes*, *Dasycladaceae*, *Girvanella* and *Epimastopora* regularly occurred in thin section (Figure 5). Algal sedimentary structures such as oncoids and boundstone textures were also identified in the thin sections as depicted in Figure 5. *Archaeolithoporella, Phylloid, Udoteacean* and *Gymnocodiacean* algae were occasionally also present. Algae appear in most of the Permian Khao Khad Formation.

CRINOIDS

Large crinoid columnals are present in thin section portray varying degrees of abrasion as shown in Figure 6. Crinoids were identified in both the Highway 21 and Siam City Cement areas. They are present in all sections except Log 1.

CORAL

The coral present in thin section were mostly identified as rugose coral of the *Waagenophyllum sp*. shown in Figure 6. They occurred as both solitary corals and parts of larger dendroid colonies. In colonies, coral are spaced between 1-5 mm apart, each with diameters between 4.5 and 7 mm. Major septa are slightly thicker than other septa and nearly touch the columella (Appendix C). Minor septa are thinner and shorter than the major septa. *Waagenophyllum sp*. occurs in the Guadalupian and Lopingian. Coral was present in Logs 2, 5, 7-9.

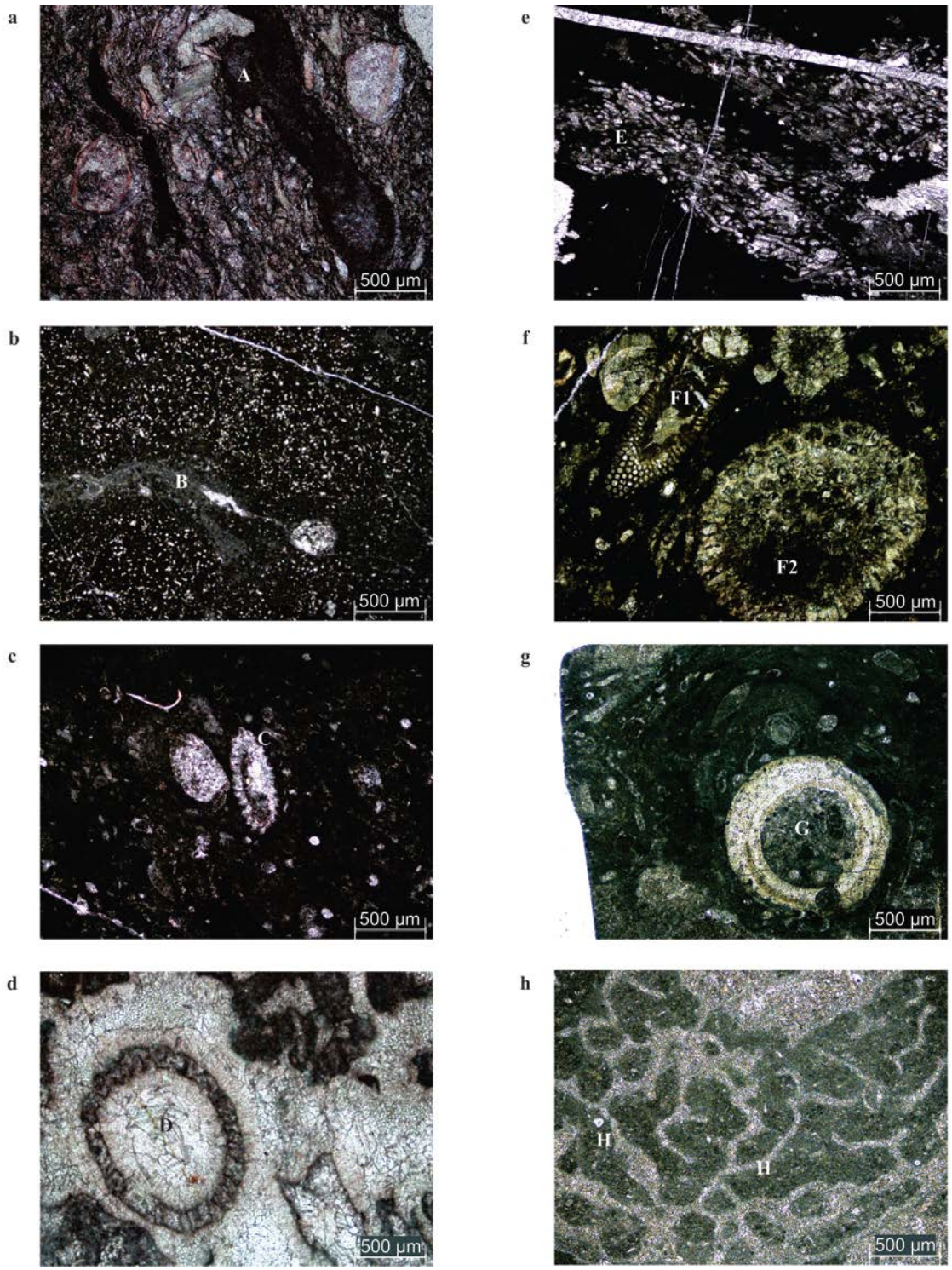

Figure 5: Distinct algal groups seen in thin section using information from Sano et al. (1990), Dawson & Racey (1993), Wendt (1997) and Flügel (2010) a) Log 5 RDT14_006B *Tubiphytes obscurus, a* cosmopolitan reef builder abundant throughout all Permian (A) b) Log 4 RDT14_057 *Tubiphytes* (B) c) Log 1 RDT14_012 *Mizzia* dasycladean algae common in Guadalupian and Lopingian shelf and back reef environments d) Log 2 RDT14_041 *Mizzia* Dasycladean algae surrounded by calcite cement (D) e) Log 1 RDT14_015 *Girvanella* (E) f) Log 2 RDT14_043 common green dasycladean algae (F1) possibly *Epimastopora* (F2) g) Log 7 RDT14_040A oncoid in an algal boundstone (G) h) Log 7 RDT14_040A algal boundstone textures.

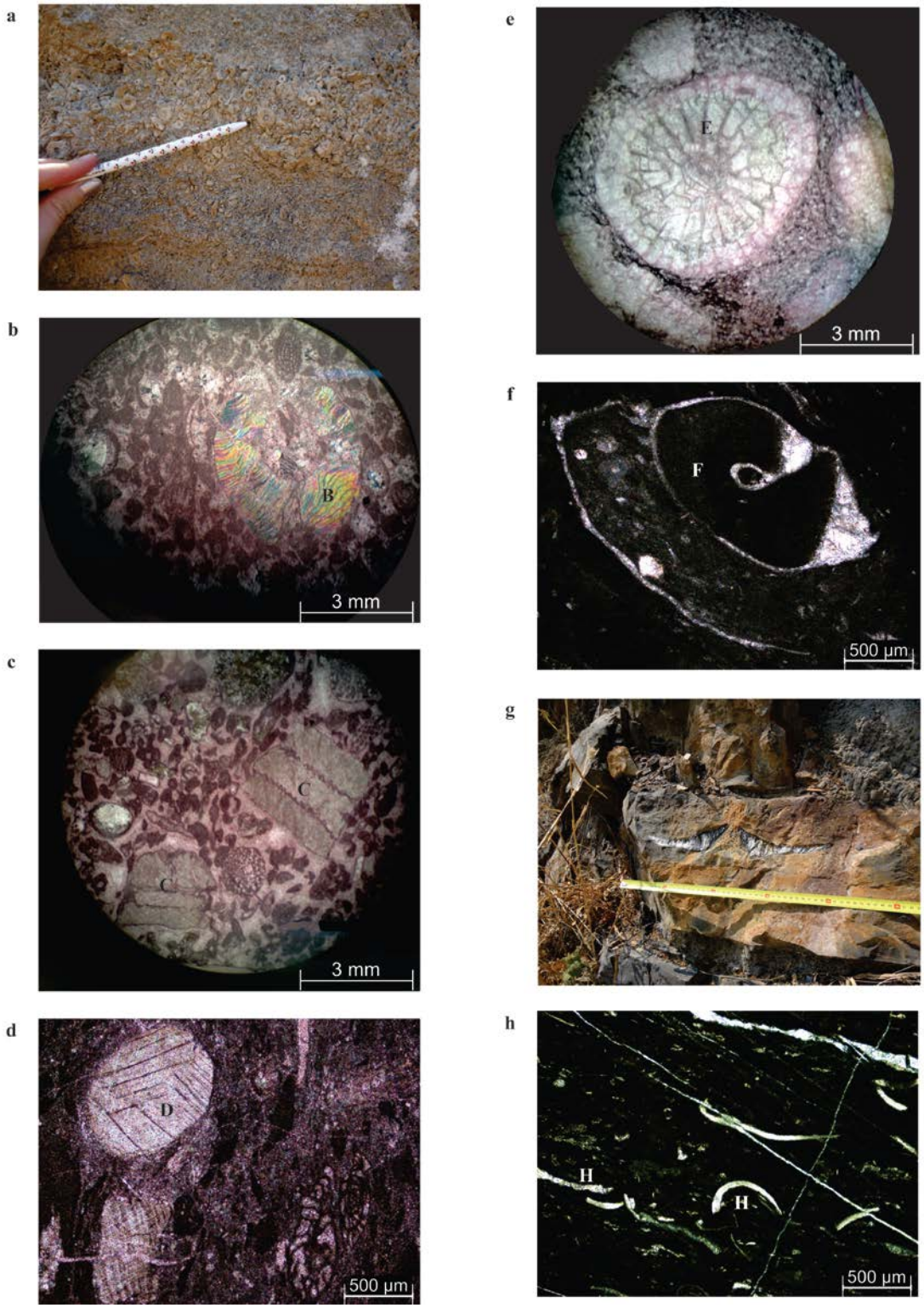

Figure 6: Other common fossils seen in thin section and in the field using information from Sorauf (1978), Fontaine et al. (1988), Dawson and Racey (1993) and Scholle and Ulmer-Scholle (2003) a) crinoidal grainstone in outcrop b) Log 2 RDT14_041 crinoid columnal close to the cup in cross-polarised light (B) c) Log 2 RDT14_041 three crinoid columnals (C) clearly shows crenulae which connect the plates d) Log 9 RDT14_051 crinoid fragments that are more abraded (D) e) Log 5 RDT14_005 Permian rugose coral *Waagenophyllum sp.* (E) f) Log 1 RDT14_012 gastropod fragment (F) g) Log 6 30 cm bivalve h) Log 4 RDT14_022A bivalve fragments (H)

GASTROPODS

Rare fragments of gastropod shells were recognised in most of the thin sections in the Highway 21 region. A typical gastropod fragment is illustrated by the gastropod in Figure 6.

BIVALVES

Bivalves were identified in the Highway 21 sections as illustrated in Figure 6. A large variety of bivalves are present, ranging in preservation from very fragmented to almost complete and vary in size between several 100 μm to 30 cm. They are common in the entire Khao Khad Formation sequence. Gregarious *alatoconchid*-bearing limestones were observed in Log 6 (Figure 6g).

Lithobiofacies of the Permian Saraburi Carbonate Sequence

Platform facies have been interpreted from the examination of logged sections to determine the type of carbonate platform (Figure 3). The environments form a continuum but can be grouped into peritidal, low-energy lagoon, high-energy middle platform to backreef, algal reef and slope to basin illustrated in Figure 3. The relationship between these facies in logged sections allows the classification of several facies associations, which are indicative of broad environments of deposition.

PERITIDAL

The peritidal zones lack coral and fusulinids and are predominantly classed as mudstones and wackestones with abundant algae (*Girvanella*) and microscopic non-fusuline foraminifera. Some algal grainstones were also present within the tidal environments. Peritidal environments occur within Log 1, 2 and the dolomitised Log 4.

Ages range from early middle Permian to middle Murgabian with possible extension into the Midian.

LAGOON

The low-energy lagoonal environment is comprised of bioturbated wackestones predominant with abundant algae including *Girvanella* and microscopic non-fusuline foraminifera (*Globivalvulina* and *Textulariida*). Algal boundstone interbeds sporadically occur along with chert nodules and lenses. The dolomitised bioturbated algal wackestones of Log 4 are characteristic of the lagoonal environment. The fossil assemblage in Log 4 implies deposition after the middle Kungurian.

OUTER PLATFORM

Massive planar-bedded dark-storm-grey wackestone with minor grainstone masses indicate the change from the lagoon and into the higher energy outer platform. Bivalves, crinoids and small foraminifera encompass the majority of the fauna.

In contrast, the backreef frequently includes non-parallel-bedded storm-grey set of wackestones, packstones and grainstones. Isolated boundstone clumps of coral families also occur like in Log 5. Fossils are disarticulated in the back reef and include each major fossil group: crinoids, fusulinids (*Nankinella, Schwagerina, Neoschwagerina* and *Gifuella* see Figure 4), bivalves (including *alatoconchids*), non-fusuline foraminifera (*Baisalina* and *Climacammina*), algae (*Tubiphytes*), coral (*Waagenophyllum* in Figure 6) and gastropods. Brachiopods, calcareous sponges and peloidal matter are also present.

The continuum of the outer platform is the interpreted depositional environment for Logs 5, 6 and 8. Chert lenses are present in the backreef of Log 5 whereas shale interbeds occur in Log 6 and 8. At a similar time to the platform interior setting, igneous activity was occurring nearby, leading to the sills found in Log 1 and 8. The fossil assemblages suggest middle to late Murgabian for the outer platform sequences.

REEF

Reef facies are dominated by algal boundstones and fusuline packstone-grainstone. Reef builders were mostly algae and fusulinids with minor foraminifera and coral building. The boundstones along Highway 21 have a dominant skeletal element of encrusting *Archaeolithoporella* and *Tubiphytes* with calcisponges and abundant syndepositional marine cements. This is consistent with descriptions by Dawson et al. (1993). The boundstone units lack fusulinids containing rare non-fusuline foraminifera. Within the fusuline packstone-grainstones, bivalves and fusulinids (including *Neofusulinella, Nankinella, Kahlerina, Armenina*) are abundant with crinoids, coral and non-fusuline foraminifera (*Cribrogenerina* and *Pachyphloia*) commonly occurring. Log 7's bivalve and fusulinid-rich grainstone with coral lenses passes west into a reef mound suggesting lateral facies change. I interpret that the platform margin was not entirely rimmed with reef builders and the margin was home to small biostromes instead. The algal reefs were identified within Logs 1, 2 and 7 and the fossil assemblages of Logs 2 and 7 depict deposition in the early to late Murgabian.

BASINAL SLOPE

The basinal slope facies are predominantly mudstones with lesser allodapic packstone-grainstone-boundstone beds. Multiple chert nodules and lenses, in addition to beds with

scoured bases along with other characteristics of mass transport are indicative of turbid debris deposits. Log 3 is the only section representative of the basinal slope environment. The fossil assemblage includes an eclectic assemblage of fragmented and abraded fossils including small crinoids pieces, fusulinids (*Neoschwagerina*), non-fusuline foraminifera (*Agathammina, Pachyphloia, Hemigordiopsis* and *Globivalvulina cyprica*) and gastropods. Together this assemblage indicates an age between Murgabian and Dzhulfian Tethyan stages.

PLATFORM (SIAM CITY CEMENT)

Logs 9 to 11 also appear to have been deposited in a platform environment.
The platform margin is characterised by dolomitised light grey grainstone is the major textural classification present in this platform margin although some mudstone and wackestone beds occur sporadically. It lacks fossil diversity with abraded crinoids dominant with minor coral, fusulinids and algae. Log 9 illustrates this platform margin. Hornblende is abundant in thin section with chert lenses appearing in outcrop. Some fossils were observed in the field to be replaced by chert. The age of the sequence could not be constrained due to the lack of fossils present in thin section.

The backreef and reef consists of pervasively dolomitised massive homogenous light pink-grey sequence. It is extremely fossiliferous although fossils were unidentifiable in the field due to the high levels of recrystallisation. The backreef and reef are distinguished within Logs 10 and 11. A diverse array of fusulinids including *Parafusulina*, *Schubertilids, Schwagerina* and *Ozawainella* were identified in thin section. They imply a late Kungurian to Guadalupian age.

AGE AND BIOSTRATIGRAPHIC CORRELATION

Age

Random errors may have occurred when constraining age as various resources gave ages using the Tethys Scale, ICS Permian Timeline or numerical age ranges. Further errors would be present if the fossil is assigned to an ICS epoch whose boundaries have since changed, i.e. the differences between timelines within Wardlaw et al. (2004), Menning et al. (2006), and Shen et al. (2013). The Tethyan Stages are sometimes referred to as the Transcaucasia or Pamirian whose boundaries between the stages vary further (Nestell and Nestell 2006, Dickins et al. 2007, Ueno and Charoentitirat 2011). For ease in this project, I have assumed that the Tethyan Murgabian and Midian are equivalent to the ICS Wordian and Capitanian respectively as suggested by Menning et al. (2006) and shown in Figure 1. This equivalence has been previously used by Wardlaw et al. (2004), Kobayashi et al. (2010).

The fossils identified in thin section were correlated using the Tethyan fusulinid zonations as no conodonts were present to be confident using the ICS Permian Timeline (Figure 1). The Tethyan Scale gave higher resolution for the fossil zonation of the Khao Khad Formation as it is the correct regional timescale for the Indochina Block (Menning et al. 2006, Ueno and Charoentitirat 2011).

Biostratigraphic Correlation

The presence of fusulinids is very helpful to recognise Permian aged sedimentary rocks; however, it is harder to establish definitive ages for sequences without prolific fusulinids. Sections (Logs 1 and 4) that predominantly contained non-fusuline foraminifera were harder to constrain ages, as they change in morphology at a slower rate than the fusulinids in the Permian.

From the fusulinids present, the sections mostly appear to be within the *Neoschwagerina simplex, N. craticulifera* and *N. margaritae* zones described in Menning et al. (2006) and depicted in Figure 1c. The *Neoschwagerinidae* present in the sections do not appear to be at the complexity of *Yabeina sp.* that are characteristic of the Capitanian/Midian discussed by Kobayashi et al. (2010) and displayed in Figure 1c. The upper section of Log 1 lacks fusulinids and therefore may still have deposition into the early Capitanian (Midian).

Overall, the fossils, especially the fusulinids, appear older in the Siam City Cement sections than the fossils along Highway 21. Nevertheless, it must be considered that the fossils are not well preserved therefore, the determination of the fossil taxonomy and age is poor.

Scattered dolomite rhombs occur within Log 4 and all three Siam City Cement sections (see Figure 7). The dolomitised peritidal environments of Log 4 and nearby Y sample location are probably the same tidal zone due to their proximity and similarity. It has been suggested that there was a sedimentary hiatus related to a worldwide marine regression in the early middle Permian, which caused a period of intense dolomitisation in the Khao Khad carbonates (Dawson and Racey 1993). This event implies that sections with intense dolomitisation were deposited prior to the early middle Permian. This is consistent with the fossil assemblages that indicate that Log 4 was deposited after the middle Kungurian and loosely constrained late Kungurian-Guadalupian Logs 10 and 11.

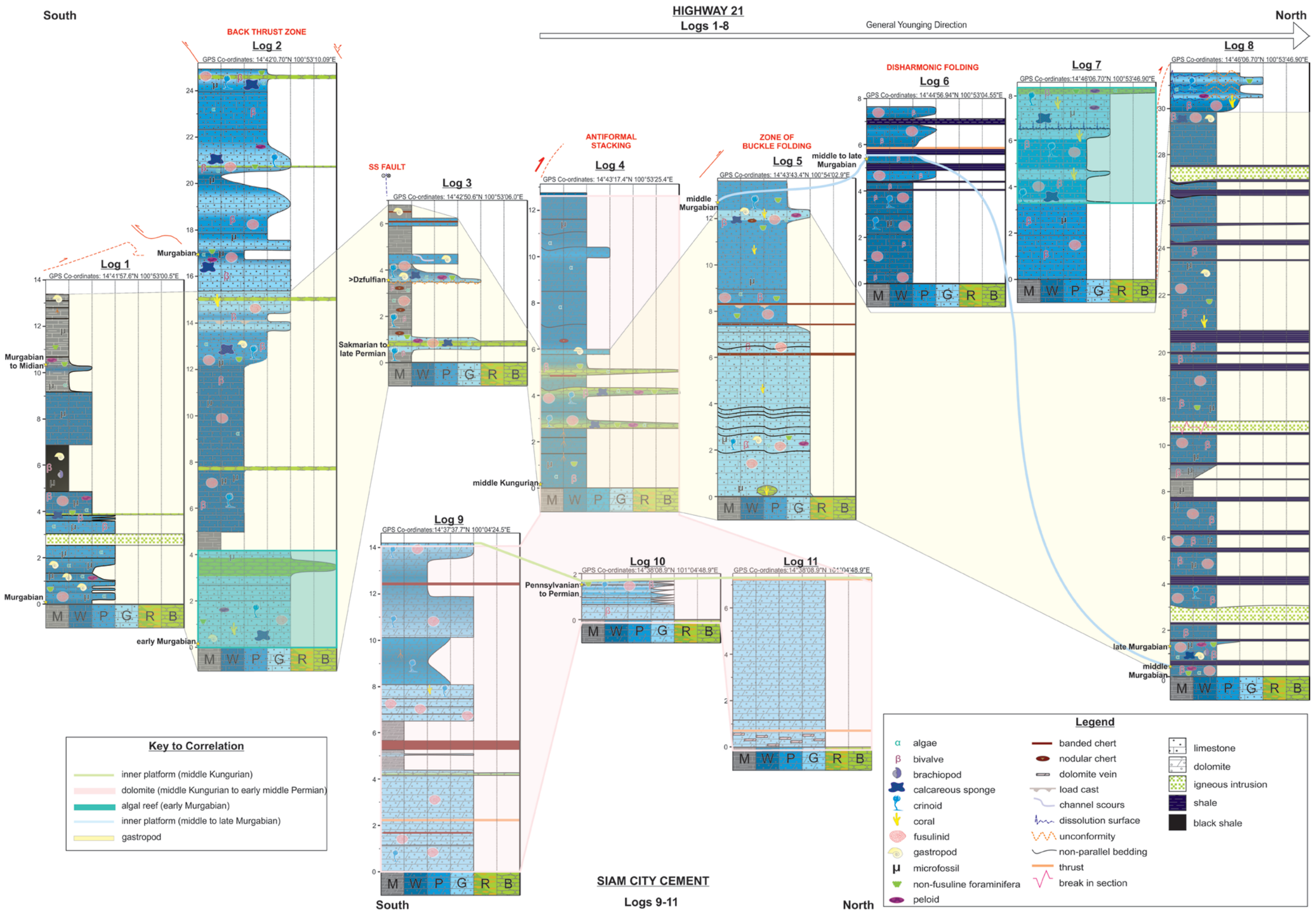

Figure 7: Fence line diagram correlating the stratigraphic logs along Highway 21 and from the Siam City Cement quarry highlighting some of the general structural trends between logs, scale on stratigraphic logs is in metres

The cooling trend throughout the Permian led to the decline of siliceous sponges, peloids and aragonitic shells (Kiessling et al. 2003, Scholle and Ulmer-Scholle 2003). The fossil assemblages indicate that most of the sequences were deposited prior to this cooling trend. Aragonitic-shelled gastropods are present at the least in the bottom of all sections south of Log 6 and 7 (shown in Figure 7). They disappear in middle Murgabian peritidal environment of Log 2, however, are still present in the late Murgabian backreef, which was perhaps warmer and more conducive for gastropods at this later time.

Logs 6 and 7 both grade from a protected inner platform lagoonal environment into an energetic middle platform to backreef. They both are also constrained to the middle to late Murgabian. The backreef environments found in the Log 5 and Z sample location may also be extensions of the same environment. In contrast, the Log 2 and Log 7 are both early Murgabian algal reefs with RDT14_041 and RDT14_038 samples appearing very similar in thin section.

There is little variance between the marginal platform of Log 9 and the backreef of Logs 10 and 11 further north. I interpret the age of these sections to be Murgabian, which is consistent with the age given in Morley et al. (2013). In contrast, the Highway 21 section can be better constrained to sections depicting sections between middle Kungurian through to the Murgabian and Midian. I interpret that the Siam City Cement sections are laterally equivalent or slightly older than the Highway 21 sections. These ages are within the ranges given previously by Baird and Bosence (1993), Dawson and Racey (1993) and Thambunya et al. (2007).

Other correlative relationships

The stratigraphic sections of Highway 21 are dominated by carbonate sequences with chert in Logs 3-5 (Figure 2). The percentage of allochems decreases up section in Log 1 and 5 unlike in Logs 6, 7 and 8 where the percentage increases up section. In contrast, the Siam City Cement sections are predominantly grainstone in composition although some micrite is present in Log 9.

There are a number of sills in the Log 1 and 8 (Figure 2). The andesitic composition of the minor dikes and sills noted in the field is consistent with previous geochemical results (Chutakositkanon, pers. data, 1996). Thin section analysis also depicted volcanic influences with volcanic hornblende occurs within the matrix of samples from Logs 3 and 9. This indicates that these sections were proximal to volcanic activity or more volcanic activity was occurring during deposition of these sequences. The sills in Logs 1 and 8 indicate that at a similar time to the Murgabian platform interior setting, igneous activity was occurring nearby. This could be associated with the Permo-Triassic Phra Ngam Diorite and Khao Yai Volcanics that are coeval with the Saraburi Group (Chutakositkanon et al. 2000, Ueno et al. 2012). As Log 1 was taken from the Khao Yai Hill locality it is probable that it may be proximal to the Khao Yai Volcanics.

PALAEOGRAPHY

Fontaine (2002) states that massive carbonate sequences represent extensive carbonate platforms; this is certainly true for the Khao Khad Formation in the Saraburi Province. The sequences studied in this project were deposited in a tropical shallow marine carbonate platform environment. However, it is difficult to determine whether they were deposited as one singular platform or multiple platform environments due to the

shortening and deformation that has since occurred. However, five carbonate facies can be identified from the examination of logged sections. The relationship between these facies in logged sections allows the classification of a number of facies associations, which are indicative of broad environments of deposition. The environments form a continuum but can be grouped into peritidal, low-energy lagoon, high-energy middle platform to backreef, algal reef and slope to basin highlighted in Figure 3.

The balanced section by Arboit et al. (pers. data, 2014) depicts the position of the facies shown in Figure 1 prior to deformation. The balanced section (Figure 8) was incorporated into my interpretation of the lithobiofacies analysis and biostratigraphy to reconstruct the palaeogeography of the margin. Most of the correlations and facies associations previously discussed were back up by the balanced section (Figure 8).

Kungurian to early middle Permian

Prior to the early middle Permian, the rocks found in Logs 4, 9-11 were deposited in peritidal and backreef environments respectively. The peritidal zones lack fusulinids and are predominantly classed as wackestones with abundant algae and microscopic non-fusuline foraminifera. After this time, there was a sedimentary hiatus and dolomitisation occurred.

Murgabian

Algal reef deposition began in the early Murgabian for Logs 2 and 7. Reef facies are dominated by algal boundstones and fusuline packstone-grainstones. Reef builders were mostly algae and fusulinids with minor foraminifera and coral building. I interpret

that the platform margin was not entirely rimmed with reef builders and the margin was home to small biostromes instead.

The fusulinids of Log 2 portray the evolution through the Murgabian from *Neofusulinella, Nankinella, Kahlerina* to *Armenina*. A Murgabian decrease in sea level is indicated between the back reef seen in RDT14_043 and the peritidal environment of RDT14_044 situated higher in the Log 2 section. The top of Log 2 returns to algal boundstones and fusuline packstone-grainstones.

Platform interior environs are inferred for middle to late Murgabian aged sequences: Logs 6, 8, Jungle and possibly Log 5 and Z sample location. Mudstone and wackestone form the quiet protected lagoon with bivalves and small foraminifera dominating the fauna. The backreef comprises of disarticulated fossils and higher energy wackestone and packstones. At a similar time to the platform interior setting igneous activity was occurring nearby leading to the sills found in Logs 1 and 8. Peritidal algal wackestones and mudstones occurred in Log 1 during this time.

Midian

The peritidal algal wackestones and mudstones of Log 1 extends into the Midian, although is poorly constrained lacking coral and fusulinids. The black shale of Log 1 (Figure 2 and 7) correlates with the Chutakositkanon et al. (2000) description of the late middle Permian transgression where the carbonate and fine-grained clastic sedimentation on the barrier was accompanied by anaerobic-starved conditions.

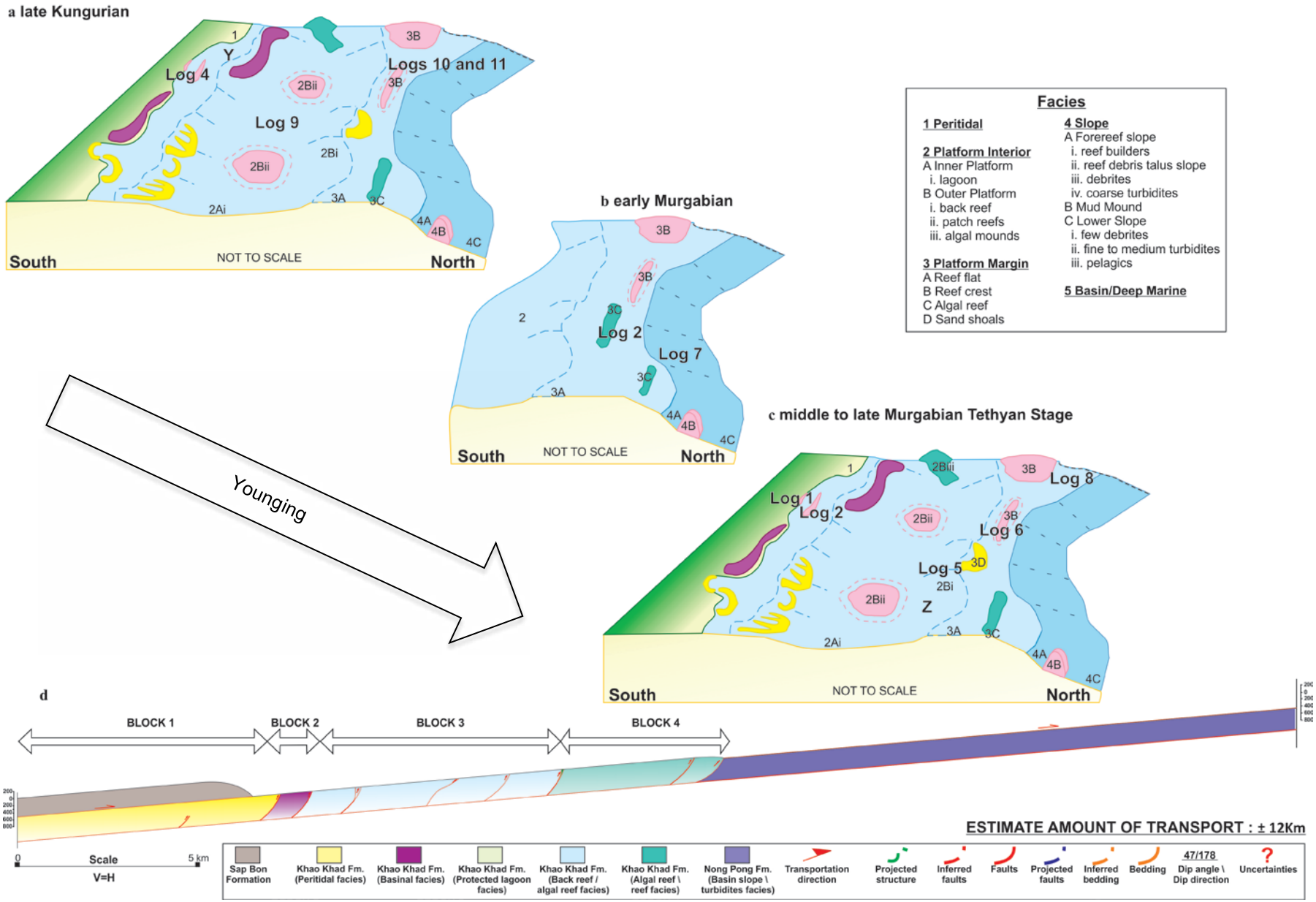

Figure 8: a-c) Interpreted Permian palaeography d) Balanced cross-section through the southern portion of the Saraburi Region, the Khao Khwang Fold-Thrust Belt adjusted from Arboit (pers. data, 2014).

IMPROVEMENTS

The analyses could be improved by integrating isotope analysis of oxygen and carbon similar to Mirzaloo (2013). Correlations with previous stratigraphic studies such as Chutakositkanon et al. (2000) would be beneficial to understand the biostratigraphic variations within the Saraburi Group at different localities. The three-dimensional simulation of stratigraphic architecture and facies distribution modelling of carbonate sediments (SIMSAFADIM) used by Bitzer and Salas (2002) could be useful to interpret palaeography.

REGIONAL TECTONIC SETTING

From my observations and interpretations, the overall direction and age of the fold-thrust belt indicates that the exposed northern foreland is younger than southern hinterland (Figure 2). Considering that this is a northward-verging fold-thrust belt, this younging down structure is what would be expected of a forward propagating fold-thrust belt. Thrust planes are visible at Logs 6, 9 and 11, which are all proximal to large-scale thrusts depicted in Figure 1. Thin-skinned deformation is suggested to have occurred within the Khao Khad Formation. There are several discrepancies to this general younging to the north trend that may be explained within the structure.

- The ages of Log 2 (early-late Murgabian) and 6 (middle to late Murgabian) appear to illustrate out of sequence thrusting.
- Logs 1 and 2 are south verging and are within the backthrust zone of the hinterland (Arboit et al. in press), which could explain why the southernmost Log 1 contains the youngest assemblages (Murgabian to Midian).

- Although Log 2 does contain some peritidal facies it is mostly part of an algal complex therefore, Figure 2 needs to be modified to indicate this.
- The older age of Log 4 (Kungurian) could be explained by the nearby strike slip fault that may have transported the sequence north. Possibly deposited further south near the late Kungurian Siam City Cement Logs 9-11.

CONCLUSIONS

The Khao Khad Formation of the study area is generally younging northwards in accordance with typical forward propagating fold-thrust belts. However, backthrusting leads to the youngest sequence being in the southern Log 1. The sequences in Logs 1-11 range from late Kungurian to Capitanian (Midian) in age with the highest proportion of assemblages classed within the Murgabian. The rapid rate of morphological change within the fusulinid taxa usually allows the identification of highly specific ages, although in the Khao Khad Formation it is harder to determine as the fossils are generally poorly preserved due to deformation. The diverse fossil assemblages were deposited in shallow marine platform environments. The environments form a continuum but can be grouped into peritidal, low-energy lagoon, high-energy middle platform to backreef, algal reef and slope to basin (Figures 3 and 8). Further structural and stratigraphic studies would assist with the further characterisation of the palaeography.

ACKNOWLEDGEMENTS

I would to formerly acknowledge:

Australian Research Council (ARC)
South Australian Chapter of the Geological Society of Australia

Mr Yot (Siam City Cement Public Company Limited)
Laainam Chaipornkaew (Petroleum Authority of Thailand (PTT))
Vladimir Davydov (Boise State University)
Aaron Hunter (Curtin University)
George Morgan (Adelaide Petrographic Laboratories Pty Ltd)

Alan Collins
Rosalind King
Francesco Arboit
Chris Morley

Morgan Blades
Robert Dew
Trudi Dew
Nicholas Harvey
Katie Howard
Madison White

REFERENCES

ARBOIT F., COLLINS A. S., KING R., MORLEY C. K. & HANSBERRY R. in press. Structure of the Sibumasu–Indochina collision, central Thailand: A section through the Khao Khwang Fold and thrust belt, *Journal of Asian Earth Sciences*.

BAIRD A. & BOSENCE D. 1993. The sedimentological and diagenetic evolution of the Ratburi Limestone, Peninsular Thailand, *Journal of Southeast Asian Earth Sciences* **8**, 173-180.

BEAVINGTON-PENNEY S. J. & RACEY A. 2004. Ecology of extant nummulitids and other larger benthic foraminifera: applications in palaeoenvironmental analysis, *Earth-Science Reviews* **67**, 219-265.

BITZER K. & SALAS R. 2002. SIMSAFADIM: three-dimensional simulation of stratigraphic architecture and facies distribution modeling of carbonate sediments, *Computers & Geosciences* **28**, 1177-1192.

BOGGS S. 2011a Carbonate and Evaporite Environments. Principles of Sedimentology and Stratigraphy: International Edition*.* 308-333, United States of America: Pearson Education, Inc.

--- 2011b Carbonate Sedimentary Rocks. Principles of Sedimentology and Stratigraphy: International Edition*.* 135-167, United States of America: Pearson Education, Inc., 5th ed.

BOUDAGHER-FADEL M. K. 2008 The Palaeozoic larger benthic foraminifera: the Carboniferous and Permian. In BOUDAGHER-FADEL M. K. ed. Developments in Palaeontology and Stratigraphy*.* 39-118: Elsevier.

BROWN G. F., BURAVAS S., CHARALJAVANAPHET J., JALICHANDRA N., JOHNSTON W. D. J., SRESTHAPUTRA V. & TAYLOR G. C. 1951. Geologic reconnaissance of the mineral deposits of Thailand, *United States Geological Survey, Bulletin* **984**, 1-183.

BUNOPAS S. 1992. Regional Stratigraphic Correlation in Thailand, *Geologic Resources of Thailand: Potential for Future Development*, 189-208.

CHONGLAKMANI C. 2001. The Saraburi Group of North-Central Thailand: Implication for Geotectonic Evolution, *Gondwana Research* **4**, 597-598.

CHUTAKOSITKANON V., CHARUSIRI P. & SASHIDA K. 2000. Lithostratigraphy of permian marine sequences, *The Island Arc* **9**, 173-187.

DAVYDOV V. I. 2013 Climate fluctuations within the western Pangean tropical shelves - the Pennsylvannian/Permian record from benthic foraminifera. In LUCAS S. G.*, et al.* eds. Part of The Carboniferous-Permian Transition*.* 73-78, Albuquerque: New Mexico Museum of Natural History.

DAWSON O., BAIRD A. & BOSENCE D. 1993. No reef-rimmed margins to the Permian carbonate platforms of Thailand, *Journal of Southeast Asian Earth Sciences* **8**, 181-186.

DAWSON O. & RACEY A. 1993. Fusuline-calcareous algal biofacies of the Permian Ratburi Limestone, Saraburi, Central Thailand, *Journal of Southeast Asian Earth Sciences* **8**, 49-65.

DICKINS J. M., ZUNYI Y. & HONGFU Y. 2007 Late Palaeozoic and Early Mesozoic Circum-Pacific Events and Their Global Correlation*.* Cambridge University Press.

DUNHAM R. J. 1962 Classification of carbonate rocks according to depositional texture. In HAM W. E. ed. Classification of carbonate rocks*.* 108-121: American Association of Petroleum Geologists Memoir.

EL TABAKH M. & UTHA-AROON C. 1998. Evolution of a Permian carbonate platform to siliciclastic basin: Indochina Plate, Thailand, *Sedimentary Geology* **121**, 97-119.

FLÜGEL E. 2010 Microfacies of Carbonates Rocks. Springer, London.

FOLK R. L. 1962. Spectral subdivision of limestone types, *Classification of Carbonate Rocks* **1**, 62-84.

FONTAINE H., LYS M. & DUC TIEN N. 1988. Some Permian corals from East Peninsular Malaysia: associated microfossils, paleogeographic significance, *Journal of Southeast Asian Earth Sciences* **2**, 65-78.

FONTAINE H. 2002. Permian of Southeast Asia: An overview, *Journal of Asian Earth Sciences* **20**, 567-588.

HADA S., KHOSITHANONT S., GOTO H., FONTAINE H. & SALYAPONGSE S. in press. Evolution and extinction of Permian fusulinid fauna in the Khao Tham Yai Limestone in NE Thailand, *Journal of Asian Earth Sciences*.

HELMCKE D. 1985. The Permo-Triassic "Paleotethys" in mainland Southeast-Asia and adjacent parts of China, *Geologische Rundschau* **74**, 215-228.

HENDERSON C. M., DAVYDOV V. I. & WARDLAW B. R. 2012 The Permian Period. In GRADSTEIN F. M., *et al.* eds. The Geologic Time Scale 2012. 653-679: Elsevier.

JAMES N. P. 1977. Facies Models 8. Shallowing-Upward Sequences in Carbonates, *1977*.

KIESSLING W., FLÜGEL E. & GOLONKA J. 2003. Patterns of phanerozoic carbonate platform sedimentation, *Lethaia* **36**, 195-226.

KOBAYASHI F., ROSS C. A. & ROSS J. R. P. 2010. Classification, phylogeny, and paleobiogeography of the new subfamily Gifuellinae and a revision of the family Neoschwagerinidae (superorder Fusulinoida); Guadalupian (Middle Permian), *The Journal of Foraminiferal Research* **40**, 283-300.

LOEBLICH A. R. & TAPPAN H. 1964 Protista 2 (Sarcodina, chiefly "Thecamoebians" and Foraminiferida). The Geological Society of America and The University of Kansas Press, U.S.A.

LUHR J. F. 2003 Earth. Dorling Kindersley Limited, London.

MACKENZIE W. S. & ADAMS A. E. 2007 A Colour Atlas of Rocks and Minerals in Thin Section. (9th edition). Manson Publishing Ltd, London.

MENNING M., ALEKSEEV A. S., CHUVASHOV B. I., DAVYDOV V. I., DEVUYST F. X., FORKE H. C., GRUNT T. A., HANCE L., HECKEL P. H., IZOKH N. G., JIN Y. G., JONES P. J., KOTLYAR G. V., KOZUR H. W., NEMYROVSKA T. I., SCHNEIDER J. W., WANG X. D., WEDDIGE K., WEYER D. & WORK D. M. 2006. Global time scale and regional stratigraphic reference scales of Central and West Europe, East Europe, Tethys, South China, and North America as used in the Devonian–Carboniferous–Permian Correlation Chart 2003 (DCP 2003), *Palaeogeography, Palaeoclimatology, Palaeoecology* **240**, 318-372.

METCALFE I. 2013. Gondwana dispersion and Asian accretion: Tectonic and palaeogeographic evolution of eastern Tethys, *Journal of Asian Earth Sciences* **66**, 1-33.

MIRZALOO M. 2013. Contrasting depositional and digenetic complexity in deep and shallow water successions in the Permian carbonates of Pak Chong region, Central Thailand. Chulalongkorn University, Bangkok.

MOORE C. H. & WADE W. J. 2013 Marine diagenetic environment. pp. 93-131.
MORLEY C. K., AMPAIWAN P., THANUDAMRONG S., KUENPHAN N. & WARREN J. 2013. Development of the Khao Khwang fold and thrust belt; implications for the geodynamic setting of Thailand and Cambodia during the Indosinian Orogeny, *Journal of Asian Earth Sciences* **62**, 705-719.
NESTELL G. P. & NESTELL M. K. 2006. Middle Permian (Late Guadalupian) foraminifers from Dark Canyon, Guadalupe Mountains, New Mexico, *Micropaleontology* **52**, 1-50.
PLUMMER H. J. 1948. Morphology of Globivalvulina, *American Midland Naturalist* **39**, 169-173.
SANO H., HORIBO K. & KUMAMOTO Y. 1990. Tubiphytes-archaeolithoporella-girvanella reefal facies in Permian buildup, Mino terrane, central Japan, *Sedimentary Geology* **68**, 293-306.
SARTORIO D. & VENTURINI S. 1988 Southern Tethys Biofacies*.* Azienda Generale Italiana Petroli (AGIP), Italy.
SCHOLLE P. A. & ULMER-SCHOLLE D. S. 2003 A Color Guide to the Petrography of Carbonate Rocks: Grains, Textures, Porosity, Diagenesis, AAPG Memoir 77*.* American Association of Petroleum Geologists, Tulsa.
SHEN S.-Z., SCHNEIDER J. W., ANGIOLINI L. & HENDERSON C. M. 2013 The International Permian Timescale: March 2013 Update. In LUCAS S. G.*, et al.* eds. Part of The Carboniferous-Permian Transition*.* Albuquerque: New Mexico Museum of Natural History.
SONE M. & METCALFE I. 2008. Parallel Tethyan sutures in mainland Southeast Asia: New insights for Palaeo-Tethys closure and implications for the Indosinian orogeny, *Comptes Rendus - Geoscience* **340**, 166-179.
SORAUF J. E. 1978. Original Structure and Composition of Permian Rugose and Triassic Scleractinian Corals, *Palaeontology* **21**, 321-339.
THAMBUNYA S., PISUTHA-ARNOND V. & KHANTAPRAB C. 2007. Depositional Environments of Permian Rocks of the Khao Khad Formation in Central Thailand, *ScienceAsia* **33**, 371-381.
TORIYAMA R. & KANMERA K. 1979 Permian fusulines from the Ratburi Limestone in the Khao Khao area, Sara Buri, Central Thailand. In KOBAYASHI T., TORIYAMA R. & HASHIMOTO W. eds. Geology and Palaeontology of Southeast Asia*.* 23-93, Tokyo: University of Tokyo Press.
TUCKER M. E. & WRIGHT V. P. 1990 Carbonate Sedimentology*.* Blackwell Publishing Ltd.
TUCKER M. E. 2001 Limestones. Sedimentary petrology: an introduction to the origin of sedimentary rocks*.* 110-165, United Kingdom: Blackwell Publishing, 3rd ed.
UDCHACHON M., BURRETT C., THASSANAPAK H., CHONGLAKMANI C., CAMPBELL H. & FENG Q. 2014. Depositional setting and paleoenvironment of an alatoconchid-bearing Middle Permian carbonate ramp sequence in the Indochina Terrane, *Journal of Asian Earth Sciences* **87**, 37-55.
UENO K. & SAKAGAMI S. 1993. Middle Permian foraminifers from Ban Nam Suai Tha Sa-at, Changwat Loei, Northeast Thailand, *Transactions and Proceedings of the Palaeontological Society of Japan*, 277-291.

UENO K. & CHAROENTITIRAT T. 2011 Carboniferous and Permian. In RIDD M. F., BARBER A. J. & CROW M. J. eds. The Geology of Thailand. 71-136, London: The Geological Society.

UENO K., MIYAHIGASHI A., KAMATA Y., KATO M., CHAROENTITIRAT T. & LIMRUK S. 2012. Geotectonic implications of Permian and Triassic carbonate successions in the Central Plain of Thailand, *Journal of Asian Earth Sciences* **61**, 33-50.

WARDLAW B. R., DAVYDOV V. I. & GRADSTEIN F. M. 2004 The Permian Period. In GRADSTEIN F. M., OGG J. G. & SMITH A. G. eds. A Geologic Time Scale 2004. 249-270, United Kingdom: Cambridge University Press.

WEIDLICH O. 2002. Permian reefs re-examined: Extrinsic control mechanisms of gradual and abrupt changes during 40 my of reef evolution, *Geobios* **35**, 287-294.

WENDT J. 1997. Aragonitic dasycladalean algae from the Upper Permian of Sichuan, China, *Lethaia* **29**, 361-368.

WRIGHT V. P. & BURCHETTE T. P. 1996 Shallow-water carbonate environments. In READING H. G. ed. Sedimentary Environments: Processes, Facies and Stratigraphy. 325-395, Victoria: Blackwell Publishing, Third ed.

WRIGHT V. P. & BURCHETTE T. P. 1998. Carbonate ramps: an introduction, *Geological Society, London, Special Publications* **149**, 1-5.

APPENDIX A: COMPLETE METHODOLOGY

FIELD WORK

The primary purpose of the fieldwork was to construct stratigraphic logs predominantly using the vast exposures of the sequence in the Saraburi Province. In addition, samples, sketches and photographs were also obtained in the field.

Stratigraphic Logging

Stratigraphic logs were taken from 11 field locations (Figure 1) to form the basis of facies interpretations and biostratigraphic correlation. A 5 m measuring tape was used to measure the sections logged. The logs were compiled in a field notebook at the scale 1:50 centimetres. Each bed was logged using Dunham (1962) shown in Figure 2 and observations of the bedding surface, matrix, fossils and preservation styles were noted. Individual symbols (Figure 3) were given to sedimentary structures and fossil groups. The relative proportion of fossils within a bed was depicted using 30% increments shown in Figure 3. If less than 30% of the fossils within the bed were gastropods only one gastropod symbol was noted for that bed. Interpretations were briefly noted initially in the field with more of an emphasis put on the field observations. A sample field log is depicted in Figure 4. Panoramic photographs were taken of each field log with other photographs and sketches taken to document the geology and fossil communities at a variety of macroscopic scales. The field logs were later digitised using CorelDRAW software (Appendix B).

No.	Log Name	Latitude (°N)	Longitude (°E)	Thickness Logged (metres)
1	Khao Yai	14 41 57.6	100 53 00.5	13.30
2	Khao Yai Detachment Fold	14 42 00.70	100 53 10.09	23.20
3	Basinal	14 42 50.6	100 53 06.0	6.78
4	Bioturbation	14 43 17.4	100 53 25.4	12.85
5	Synform	14 43 43.4	100 54 02.9	13.70
6	Jungle	14 44 09.63	100 53 43.71	7.53
7	Quarry of the North Above the Thrust	14 46 06.7	100 53 46.9	8.25
8	Quarry of the North Below the Thrust	14 46 06.7	100 53 46.9	24.79
9	Alum Shale	14 37 37.7	101 04 24.5	13.41
10	Middle Ridge Log A	14 38 08.9	101 04 48.9	1.67
11	Middle Ridge Log B	14 38 08.9	101 04 48.9	7.21
	Total			**132.69**

Figure 1: Locations of the stratigraphic logs

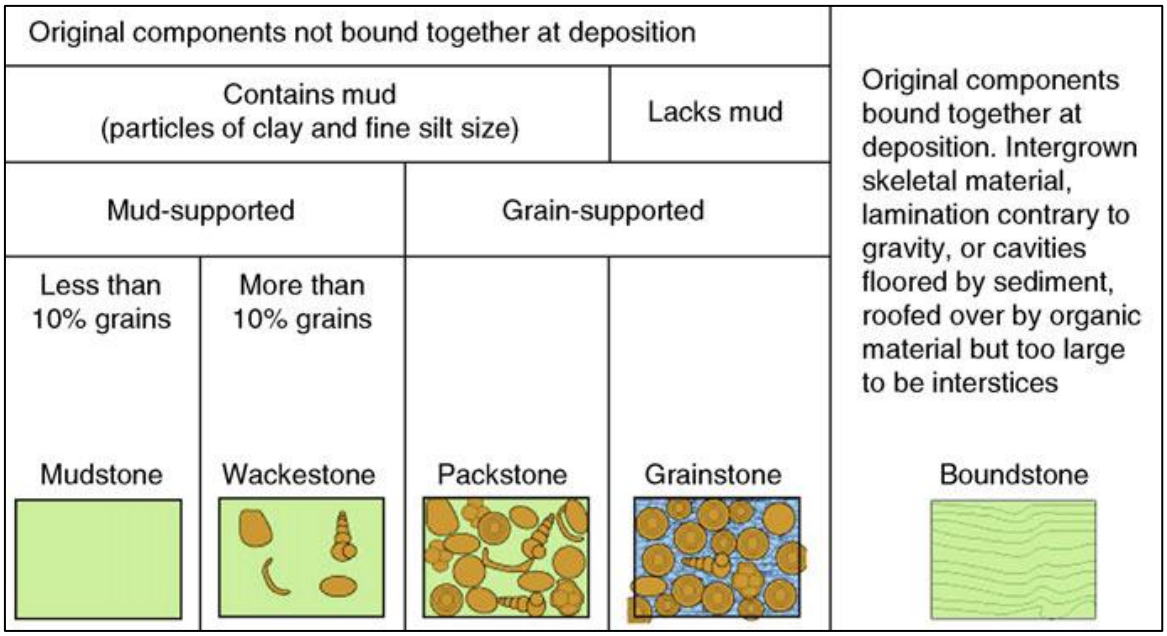

Figure 2: Dunham's 1962 classification of carbonate rocks. Taken from: Kendall and Flood (2011)

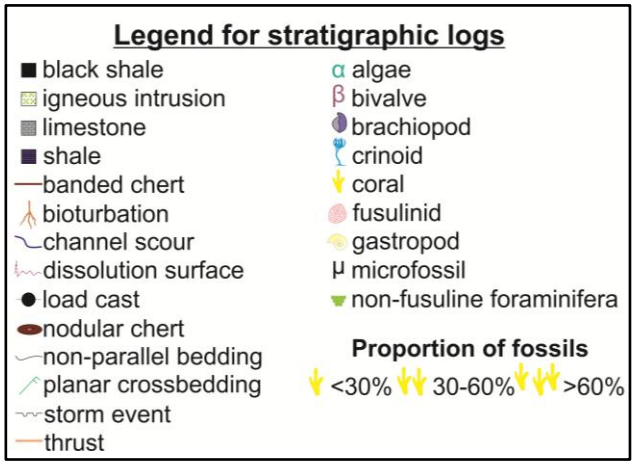

Figure 3: Legend of symbols used for the stratigraphic logs

Observations	Sample and Photo Numbers	Metre scale 1cm = 50 cm						Symbols	Interpretations
Undulating bedding surface 40-90cm, dark mud matrix, mm size white fossils, articulate gastropods, dark algae	Photo 226 RDT14_005		Mudstone	Wackstone	Packstone	Grainstone	Rudstone	Boundstone	α α	Life assemblage of a low energy algal mat or shallow lagoon

Figure 4: Layout of field notebook with example field log

Sample Collection

Samples were taken approximately every 2-3 metres or when a major stratigraphic change was observed. The samples position along the stratigraphy was marked on the log as demonstrated in Figure 4. Several samples were also taken from locations were logs were not practicable or worthwhile (Figure 5). Each sample and its fossil assemblage was described and numbered according to the format in Figure 6. Overall, 63 samples were collected from the field area.

Symbol	Location Name	Latitude (°N)	Longitude (°E)
Z	Fold Imbrication	14 43 49.5	100 53 25.7
-	Lake Quarry	14 40 03.3	100 56 29.2
Y	Tidal	14 43 26.9	100 52 57.5

Figure 5: Sample locations were logs were not taken

RDT14_...
Physical Description
Colour: matrix and fossils
Fossil Scale: size, length, width and diameter
Fossil Type
Disarticulated (shell) or fragmented (not shell)

Preservation
Original shell or replaced
Assemblage: death or life
Abrasion
Borers? Indicate at surface
>1 relationship alignment

Figure 6: Sample description format

THIN SECTION PREPARATION

32 samples (Figure 7) were prepared by Adelaide Petrographic Laboratories Pty Ltd, using the following procedure:

1. A 25 mm x 55 mm x 8 mm thick slab was cut using a 250 mm diameter rock-cutting saw blade with a continuous diamond rim.
2. A top surface on the slab is manually ground flat on a bench-mounted, horizontal diamond grinding wheel Habit-brand grit size 64.
3. The coarse ground top surface is warmed on a hot plate (at 50^{o}C), and the top coarse-ground surface is impregnated with an epoxy mix of Araldite LC191 resin, with HY951 hardener, ratio 8:1.
4. The top surface is manually more finely ground flat using 600 SiC grit on a zinc-lap or glass plate, water is utilised as a lubricant.
5. This flat finely ground surface is cleaned, checked manually for "perfection". If open porosity is still exposed another veneer of epoxy is applied.
6. The ground surface is glued onto a clean, dry glass slide, ground to a known thickness, using a UV curing, cyanoacrylate liquid adhesive "Loctite Impruv 36331". Exposure to a UV light of the glued interface through the back of the glass slide cures the adhesive in 2 to 3 minutes. This is a permanent bond, and the rock (or eventual wafer) cannot be ever separated from the glass.
7. The block mounted on glass is cut off using a trim saw with a thin continuous diamond rimmed sawblade (Diatrenn E2-G), to leave a thickness of about 1 mm of the sample slab (glued onto the glass slide), with the top surface exposed for further processing.
8. The 1 mm slab thickness is further ground down on a diamond wheel (Habit D76) held within a special jig attachment by vacuum, using water as a lubricant. This reduces the slab thickness stuck on the glass, to a wafer of about 120 micron (0.12 mm).
9. The glass slide of known thickness with the glued-on rock wafer is then loaded and held in place on the face of a special jig, and lapped flat on a Logitech machine, to a final petrographic thickness of the rock wafer, of 30 micron, using 600 SiC grit as the grinding abrasive, and water as a lubricant.
10. When the Logitech lapping cycle is finished, the quality of the wafer on the glass is assessed, also optically checked for the required 30 micron thickness,
11. When optics and quality are confirmed, the section is cleaned and covered with a glass coverslip, using the same UV curing adhesive as listed above. Again this is a permanent fix, i.e. the coverslip cannot be removed.
12. The final thin section is again cleaned and labelled.

Sample Number	Suffix	Log Number	Location
17		3	Basinal
18		3	Basinal
20		4	Bioturbation
21		4	Bioturbation
22	A	4	Bioturbation
56		4	Bioturbation
57		4	Bioturbation
41		2	Detachment Fold Khao Yai
43		2	Detachment Fold Khao Yai
44		2	Detachment Fold Khao Yai
45		2	Detachment Fold Khao Yai
46		2	Detachment Fold Khao Yai
47	B	9	Eagle Cement Alum Shale
50		9	Eagle Cement Alum Shale
51		9	Eagle Cement Middle Ridge A
31		Z	Fold Imbrication
12		1	Khao Yai
14	A	1	Khao Yai
15		1	Khao Yai
37	B	7	Quarry of the North Above the Thrust
38	B	7	Quarry of the North Above the Thrust
40	A	7	Quarry of the North Above the Thrust
23		8	Quarry of the North Below the Thrust
24		8	Quarry of the North Below the Thrust
34	A	8	Quarry of the North Below the Thrust
34	B	8	Quarry of the North Below the Thrust
5		5	Synform
6	B	5	Synform
10	C	5	Synform
10	A	5	Synform
11		5	Synform
30		Y	Tidal

Figure 7: Samples that were sectioned for optical microscopy

CARBONATE STAINING

All staining was conducted by Adelaide Petrographic Laboratories Pty Ltd, using the following chemicals and procedure:
Chemicals required:
Analytical hydrochloric acid HCl
Distilled water
Potassium ferricyanide $K_3Fe(CN)_6$ (PF)
Alizarin Red or sodium alizarin sulphonate ($CO.C_6H_4.CO.C_6H\ (OH)_2.SO_3\ Na + H_2O$ (ARS)

Preparation:

- Dilute the HCl to 1.5% by adding 15 millilitres of acid with a litre of distilled water.
- Make up a mixture of one litre of Alizarin Red using 2 grams of alizarin red to a litre of water (which is 1.5% HCl distilled water solution).
- Make up one litre of potassium ferricyanide using 20 grams of potassium ferricyanide per litre of 1.5%HCl distilled water.
- The staining involves two procedures:

Part 1

- Make up a mix of the Alizarin Red and the potassium ferricyanide at a ratio of 3 parts Alizarin Red to 2 parts Potassium ferricyanide. In the photo tray (or slide racks), cover samples in the 3:2 mixture and gently agitate for a period of 45 to 60 seconds.
- Remove samples and wash gently but thoroughly in running tap water.

Part 2

- Immediately after Part 1, submerge samples in the solution consisting of only Alizarin Red. Agitate for 15 to 20 seconds.
- Wash all samples again and then dry using compressed air.
- The staining procedure leads to various colour responses from carbonate minerals, which are depicted in Figure 8.

Carbonate		Staining Response		
		ARS	PF	ARS+PF
Hexagonal	Calcite	Pink orange	None	Pink orange
	Ferroan Calcite	Pink orange	Blue	Lilac mauve, royal blue, light scarlet
	Dolomite	None	None	None
	Ferroan Dolomite	Pale mauve	Blue turquoise	Blue turquoise
	Siderite	None	None	None
	Magnesite	None	None	None

	Rhodochrosite	None	Pale brown	Pale brown
Orthorhomic	Aragonite	Pink orange	None	Pink orange
	Witherite	Red	None	Red
	Cerussite	Mauve	None	Mauve

Figure 8:Response of common rock forming carbonate minerals to staining with Alizarin Red S / potassium ferricyanide stain taken from Ayan (1965) and Dickson (1966).

OPTICAL MICROSCOPY

The 32 samples were analysed using optical microscopes. The Olympus BX51microscope was used for majority of section photography and analysis; although, the Nikon OPTIPHOT2-POL microscope was used to check the polarisation characteristics and for sections that needed a wider lens i.e. RDT14_005 with 6 mm diameter coral. All sections were characterised using both the Dunham (1962) (Figure 2) and Folk (1962) (Figure 10) classifications. The proportion of fossils: rare, common or abundant were estimated from the thin sections.

Section Number: **Location:** **Date:**

Grains		
Type:	bioclasts /ooids / peloids / intraclasts /aggregates	
Size:		
Mineralogy:		
	Carbonate Mineral	**ARS + PF Stain**
	Calcite	Pink orange
	Ferroan Calcite	Lilac mauve, royal blue, light scarlet
	Dolomite	None
	Ferroan Dolomite	Blue turquoise
	Siderite	None
	Magnesite	None
	Rhodochrosite	Pale brown
	Aragonite	Pink orange
	Witherite	Red
	Cerussite	Mauve
Fossils:	α algae β bivalve brachiopod crinoid coral fusulinid gastropod μ microfossil non-fusuline foraminifera calcareous sponge peloid	
Micrite (lime mud) Grains < 4 μm		
Presence:		almost opaque brown colour
Origin?		
Cements Grains >10 μm		
Type:	fibrous/bladed calcite; syntaxial overgrowths; drusy/poikilotopic calcite spar	
Geometry:	meniscus / isopachous / pore-filling	
Spar Mineralogy:	non-ferroan, ferroan or zoned	
	Carbonate Mineral	**ARS + PF Stain**
	Calcite	Pink orange
	Ferroan Calcite	Lilac mauve, royal blue, light scarlet
	Dolomite	None
	Ferroan Dolomite	Blue turquoise
	Siderite	None
	Magnesite	None
	Rhodochrosite	Pale brown
	Aragonite	Pink orange
	Witherite	Red
	Cerussite	Mauve
Original Mineralogy:	aragonite / calcite / high-Mg calcite	
Timing:	Cement precipitation: early / late and pre or post compaction	
Replacement, recrystallisation and neomorphism		
Replacement Mineralogy:	chert / phosphate replacing calcite grains / micrite / cement	
Neomorphism:	aragonitic shells / ooids / cements replaced by calcite micrite replaced by microspar	
Timing:	pre / post compaction	

Dolomitisation			
Type:	scattered rhombs / pervasive dolomitisation		
Fabric control:	grains / matrix preferentially dolomitised		
Texture:			
Crystal:	Shape:	Size:	Zonation: Yes / No
Timing:	early / late; pre / post compaction; pre / post to calcite diagenesis		
Dedolomitisation:			
Compaction			
Mechanical:	broken bioclasts / broken micrite envelope / spalled oolitic coating / early cement		
Chemical:	sutured contacts; pre / post burial spar cementation; styolites; through-going pressure dissolution seams		
Porosity			
Type:	Primary: intergranular / intragranular / cavity / growth Secondary: fracture / dissolutional / intercrystalline (through dolomitisation)		
Classify			
Dunham:			
Folk:			
Diagenetic Alteration:	partly dolomitised / silicified / recrystallised		
Depositional Environment			
Grain Type/texture:	G: mod to high E shallow subtidal; M-W: low E lagoonal / outer shelf / ramp		
Bioclasts:	open-marine / restricted / deep-water / shallow / non-marine		
Interpretation:			
Diagenesis			
Processes:	early (near-surface) / late (burial)		
Timing:	cement: early / late and pre or post compaction		
Compaction:	Degree of compaction		
Dolomitisation:	partly dolomitised / silicified / recrystallised		
Pore Chemistry:	marine / freshwater; Eh / pH from non / ferroan calcite / dolomite		
Succession of diagenetic events:			

Figure 9: Form used to describe each thin section adjusted from Tucker (2001)

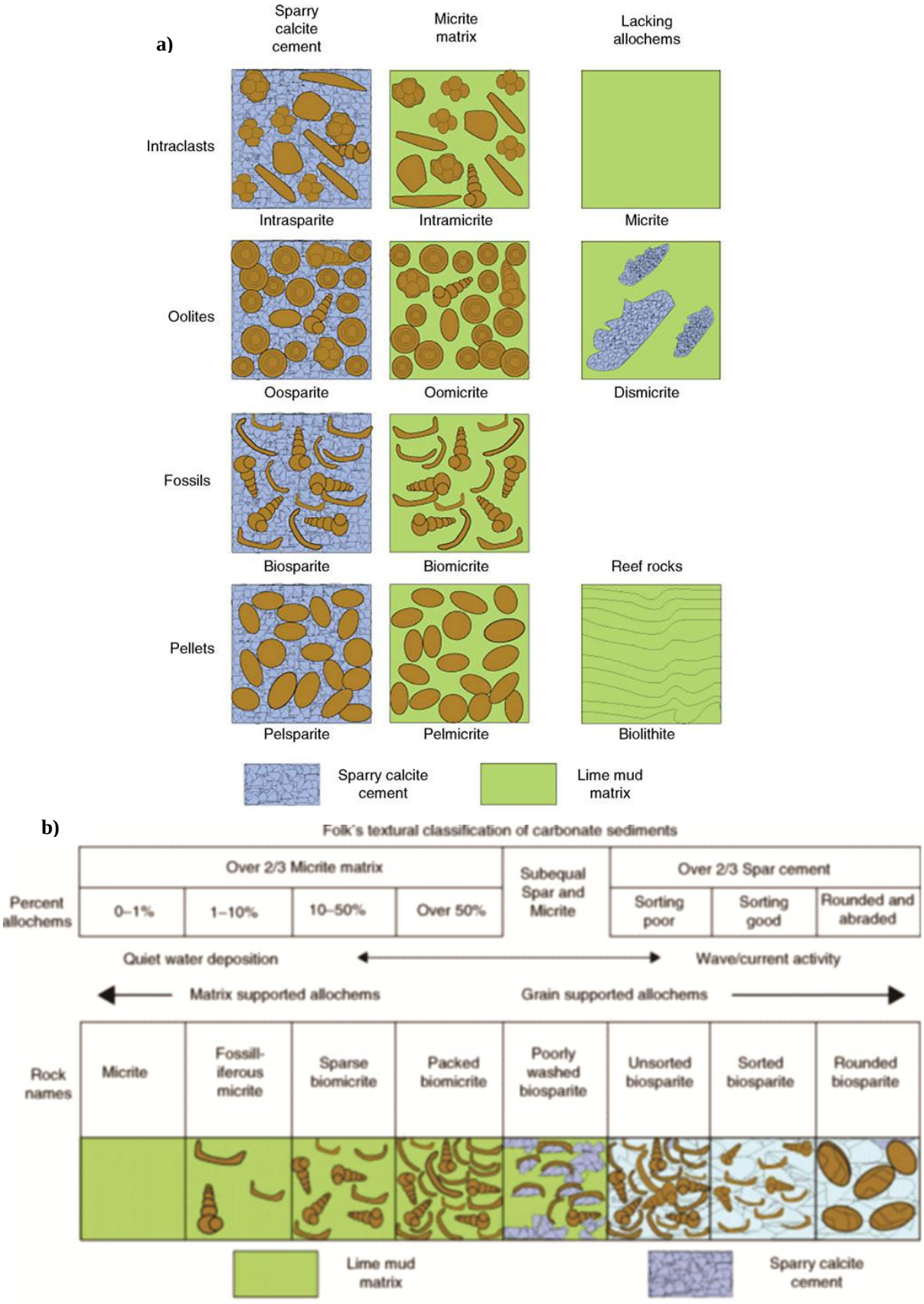

Figure 10 a) Folk's 1962 classification of carbonates b) Folk's 1962 textural spectrum for carbonate sediments. Adjusted from: Kendall and Flood (2011) and Scholle and Ulmer-Scholle (2003)

MACROFACIES CROSSCHECK

Hand specimens of some samples were cut or recut to crosscheck field carbonate classifications. Some samples were cut with the rocksaw to augment the descriptions for locations where thin sections were not created or to crosscheck the presence of certain fossils. A form similar to the form for thin section analysis was created as shown in Figure 11.

Section Number: **Location:** **Date:**

Grains			
Type:	bioclasts /ooids / peloids / intraclasts /aggregates		
Size:			
Mineralogy:			
Articulation:	Shell: articulate / disarticulated	Not shell: fragmented or whole	
Fossils:	α algae β bivalve brachiopod crinoid coral	fusulinid gastropod μ microfossil non-fusuline foraminifera	calcareous sponge peloid
Micrite (lime mud) Grains < 4 μm			
Presence:		almost opaque brown colour	
Origin?			
Cements Grains >10 μm			
Type:	fibrous/bladed calcite; syntaxial overgrowths; drusy/poikilotopic calcite spar		
Geometry:	meniscus / isopachous / pore-filling		
Spar Mineralogy:	non-ferroan, ferroan or zoned		
Original Mineralogy:	aragonite / calcite / high-Mg calcite		
Timing:	Cement precipitation: early / late and pre or post compaction		
Replacement, recrystallisation and neomorphism			
Replacement Mineralogy:	chert / phosphate replacing calcite grains / micrite / cement		
Neomorphism:	aragonitic shells / ooids / cements replaced by calcite micrite replaced by microspar		
Timing:	pre / post compaction		
Dolomitisation			
Type:	scattered rhombs / pervasive dolomitisation		
Fabric control:	grains / matrix preferentially dolomitised		
Texture:			
Crystal:	Shape:	Size:	Zonation: Yes / No
Timing:	early / late; pre / post compaction; pre / post to calcite diagenesis		
Dedolomitisation:			
Compaction			
Mechanical:	broken bioclasts / broken micrite envelope / spalled oolitic coating / early cement		
Chemical:	sutured contacts; pre / post burial spar cementation; styolites; through-going pressure dissolution seams		
Porosity			
Type:	Primary: intergranular / intragranular / cavity / growth Secondary: fracture / dissolutional / intercrystalline (through dolomitisation)		

Classify	
Dunham:	
Folk:	
Diagenetic Alteration:	partly dolomitised / silicified / recrystallised
Depositional Environment	
Grain Type/texture:	G: mod to high E shallow subtidal; M-W: low E lagoonal / outer shelf / ramp
Bioclasts:	open-marine / restricted / deep-water / shallow / non-marine
Interpretation:	
Diagenesis	
Processes:	early (near-surface) / late (burial)
Timing:	cement: early / late and pre or post compaction
Compaction:	Degree of compaction
Dolomitisation:	partly dolomitised / silicified / recrystallised
Pore Chemistry:	marine / freshwater; Eh / pH from non / ferroan calcite / dolomite
Succession of diagenetic events:	

Figure 11: Form used to describe each thin section adjusted from Tucker (2001)

Fossil Identification

Typical fossils for my study area are identified and described by Dawson and Racey (1993). Other common fossils were characterised using Sartorio and Venturini (1988), Scholle and Ulmer-Scholle (2003), Flügel (2010). Foraminiferal identification was completed in accordance with descriptions and images given in Loeblich and Tappan (1987) and BouDagher-Fadel (2008a). These descriptions were supplemented by classification from Haynes (2001), BouDagher-Fadel (2008b), Bellier et al. (2010).

Correlating Sections

The age of each sequences can be determined using the fossil assemblages. Variations and similarities in assemblages were observed within and between sections. The differences and similarities between sections could be associated to visualise potential depositional settings. The facies and their associations were then used to reconstruct a model for the depositional setting of the Khao Khad Formation during the Permian. The examination of similar depositional models by Dawson and Racey (1993), Thambunya et al. (2007), Flügel (2010) were useful in the interpretation of the study area's palaeography. The correlations interpreted and the construction palaeographic models were digitised using CorelDRAW software.

APPENDIX B: COMPLETE STRATIGRAPHIC SECTIONS

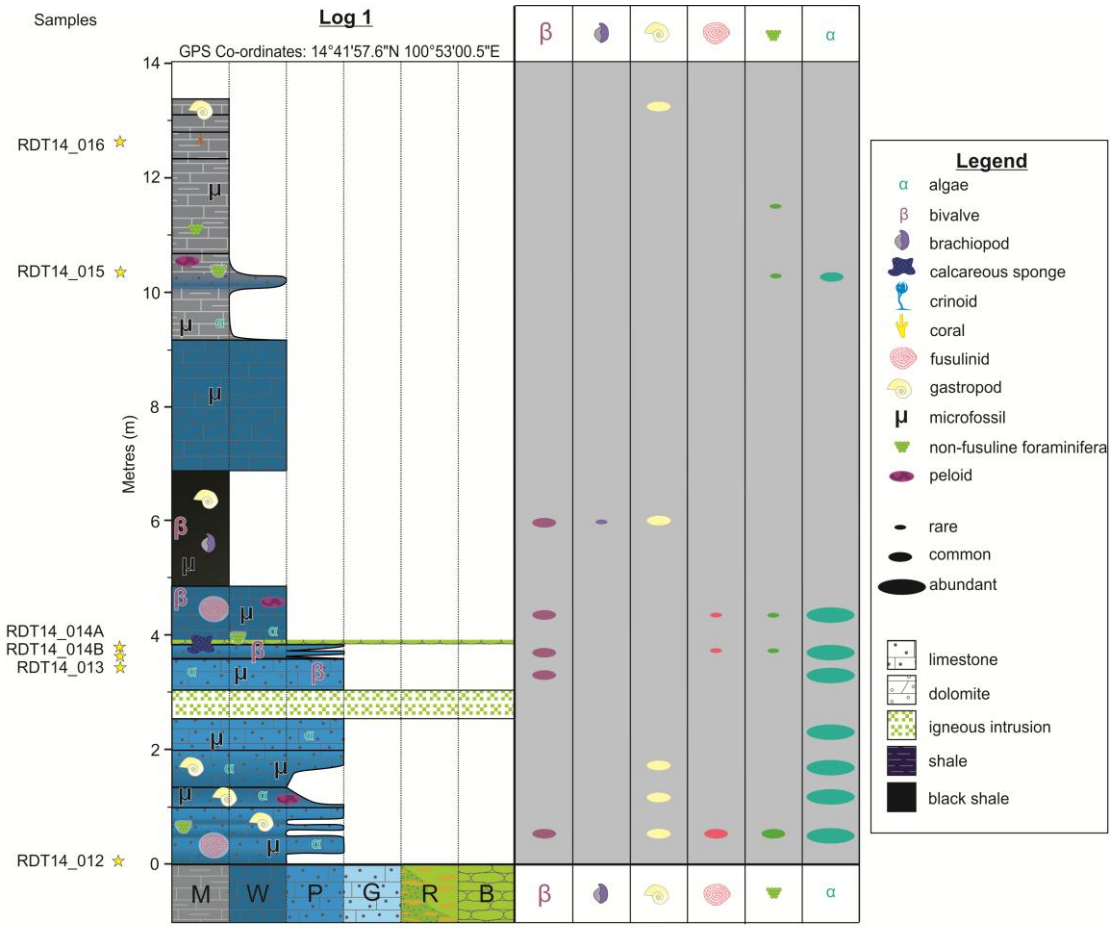

Stratigraphic log of Log 1: the Khao Yai Hill region incorporating both macrofacies and microfacies analyses. M=Mudstone, W=Wackestone, P=Packstone, G=Grainstone, R=Rudstone, B=Boundstone

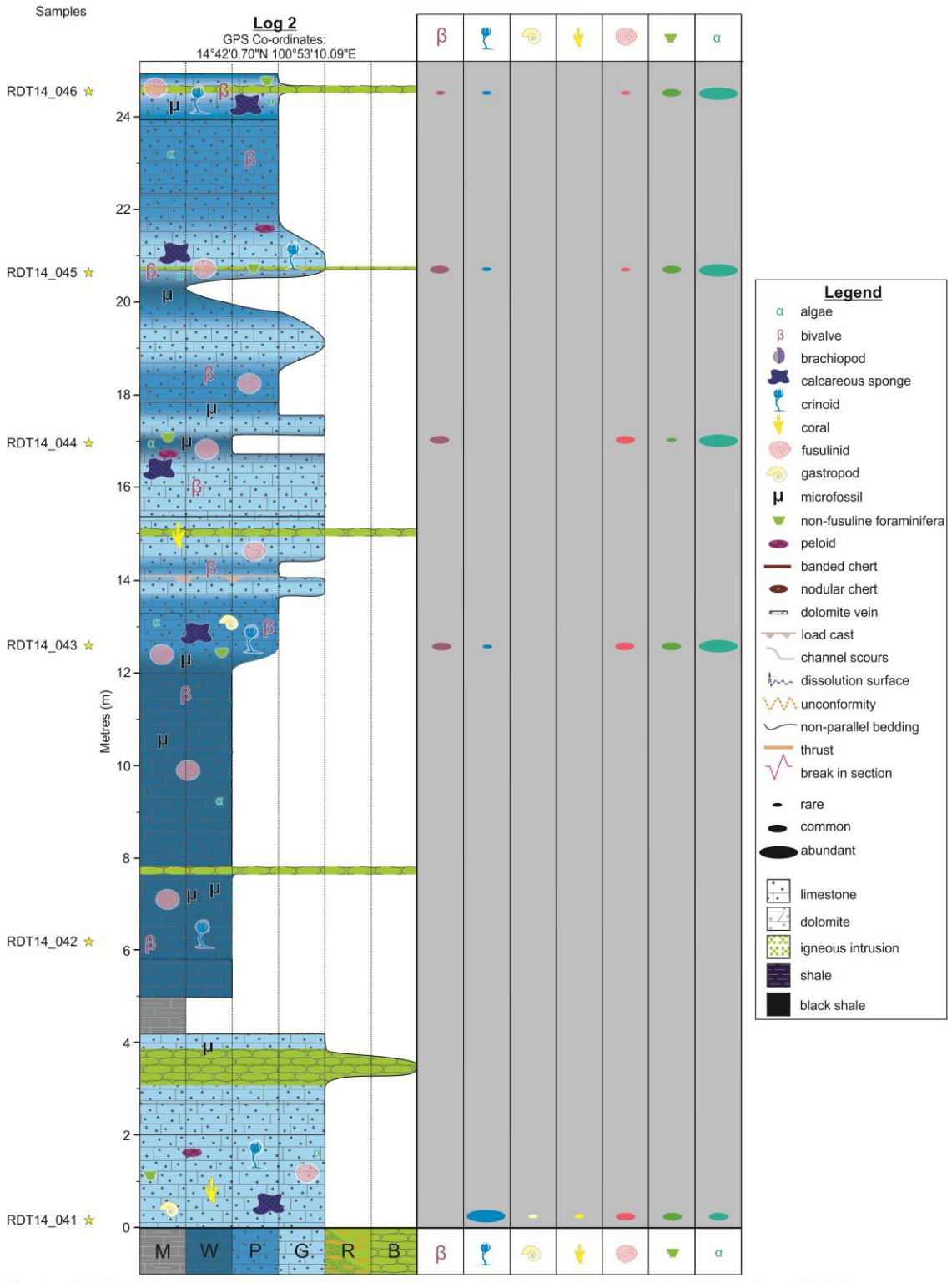

Stratigraphic Log 2: the Khao Yai Detachment Fold region incorporating both macrofacies and microfacies analyses. M=Mudstone, W=Wackestone, P=Packstone, G=Grainstone, R=Rudstone, B=Boundstone

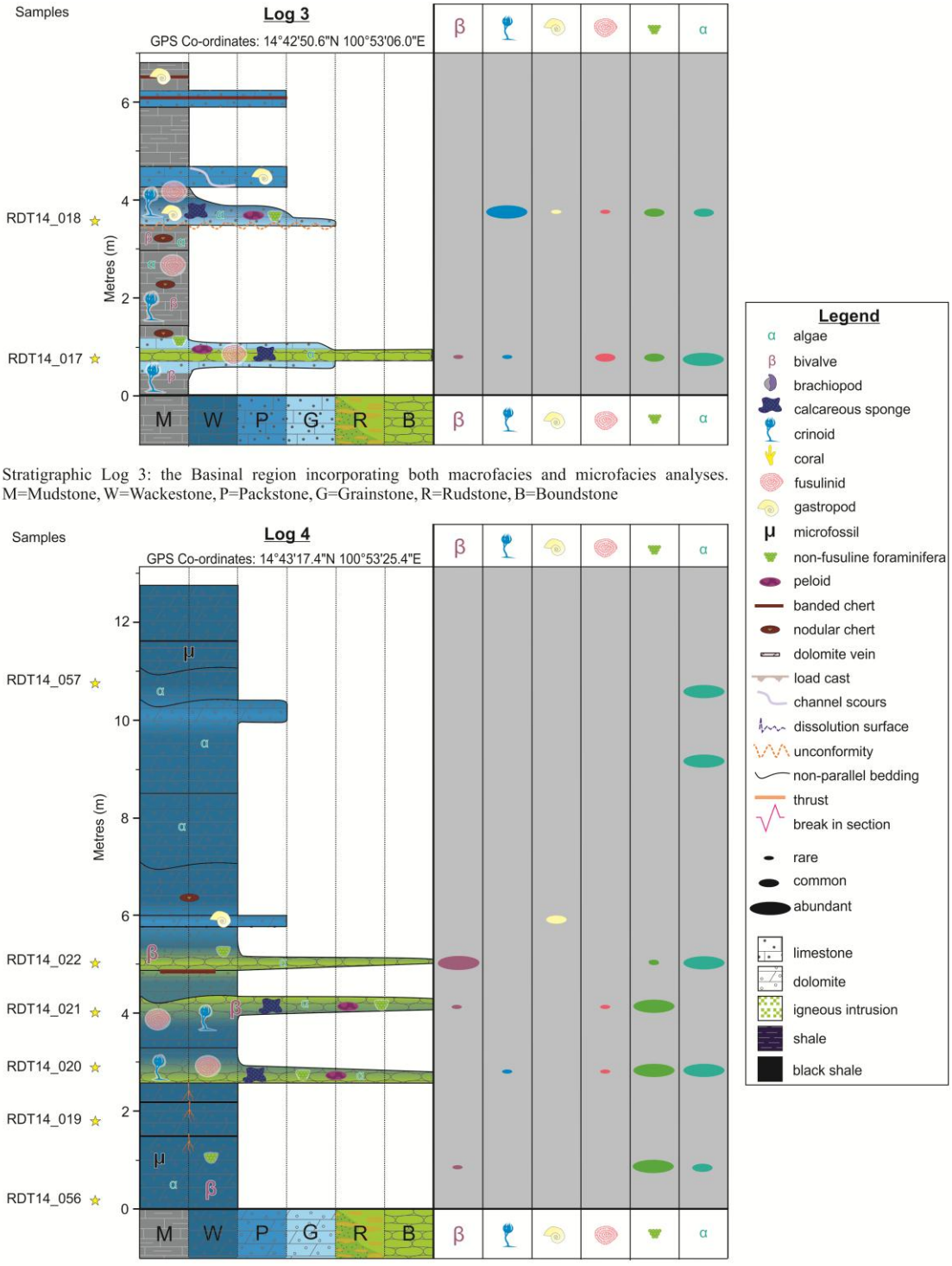

Stratigraphic Log 3: the Basinal region incorporating both macrofacies and microfacies analyses. M=Mudstone, W=Wackestone, P=Packstone, G=Grainstone, R=Rudstone, B=Boundstone

Stratigraphic Log 4: the Bioturbation region incorporating both macrofacies and microfacies analyses. M=Mudstone, W=Wackestone, P=Packstone, G=Grainstone, R=Rudstone, B=Boundstone

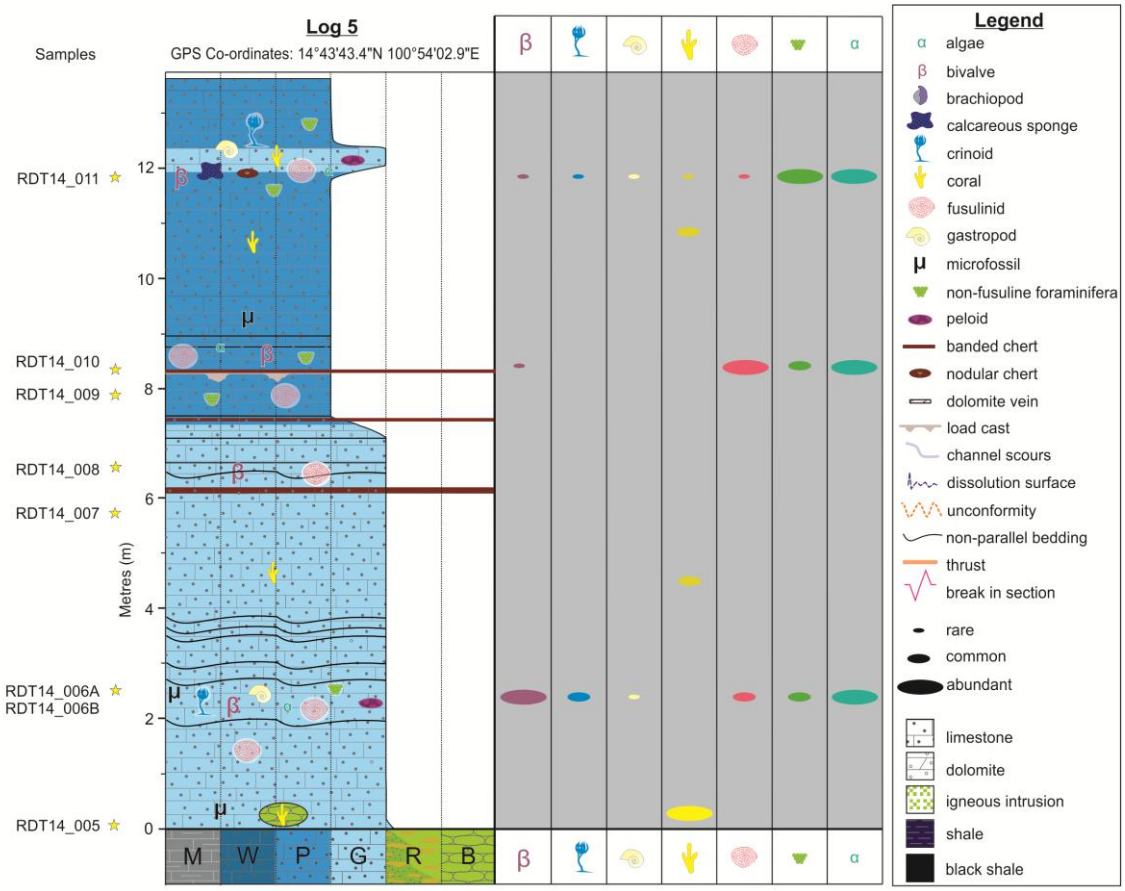

Stratigraphic Log 5: the Synform region incorporating both macrofacies and microfacies analyses. M=Mudstone, W=Wackestone, P=Packstone, G=Grainstone, R=Rudstone, B=Boundstone

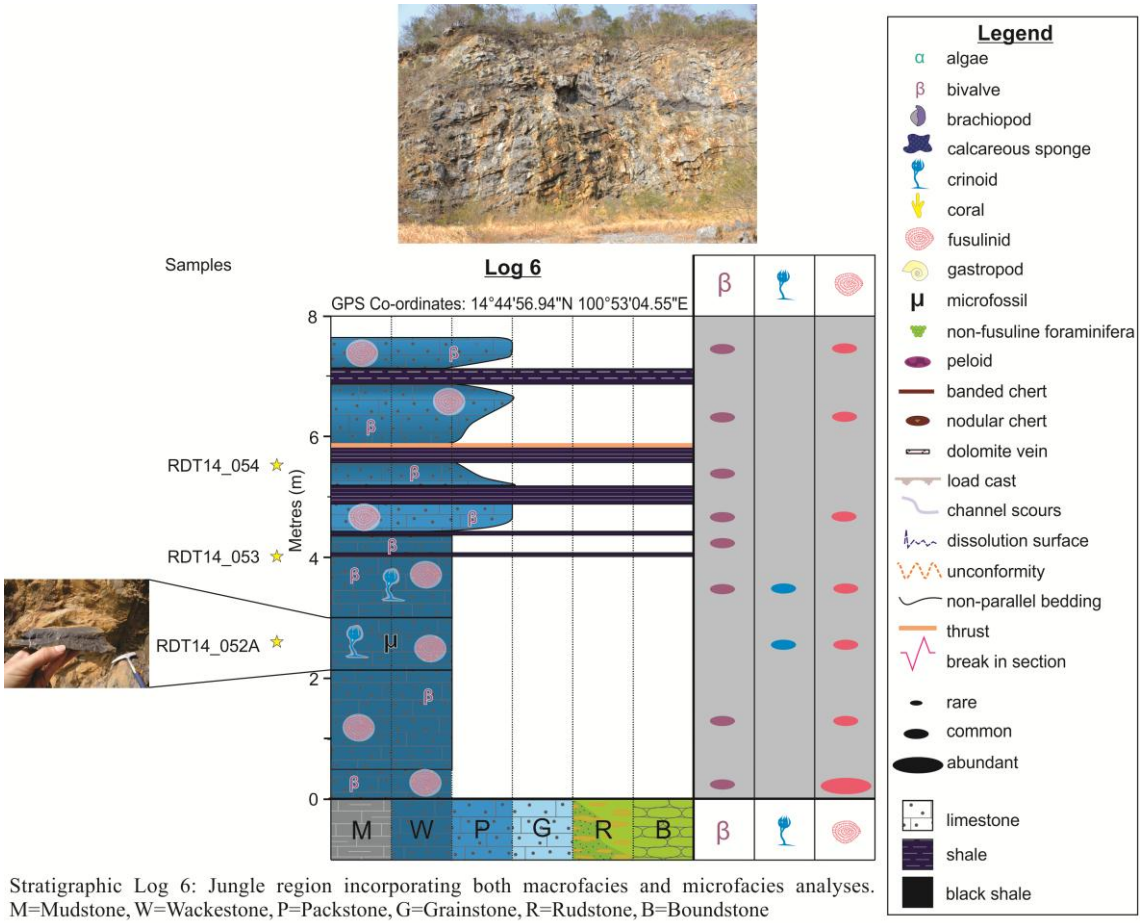

Stratigraphic Log 6: Jungle region incorporating both macrofacies and microfacies analyses. M=Mudstone, W=Wackestone, P=Packstone, G=Grainstone, R=Rudstone, B=Boundstone

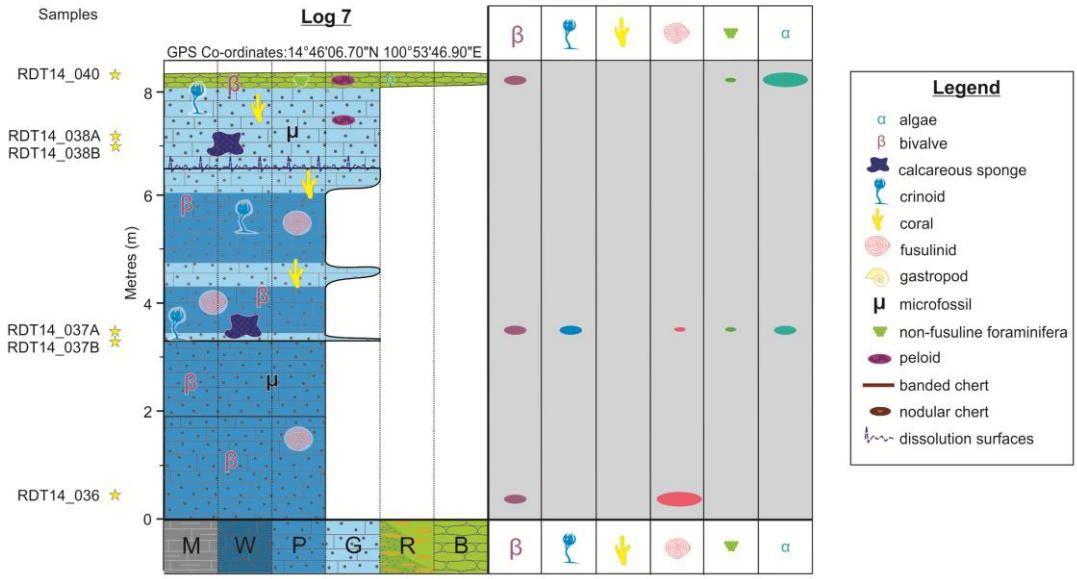

Stratigraphic Log 7: the Quarry of the North Above the Thrust region incorporating both macrofacies and microfacies analyses. M=Mudstone, W=Wackestone, P=Packstone, G=Grainstone, R=Rudstone, B=Boundstone

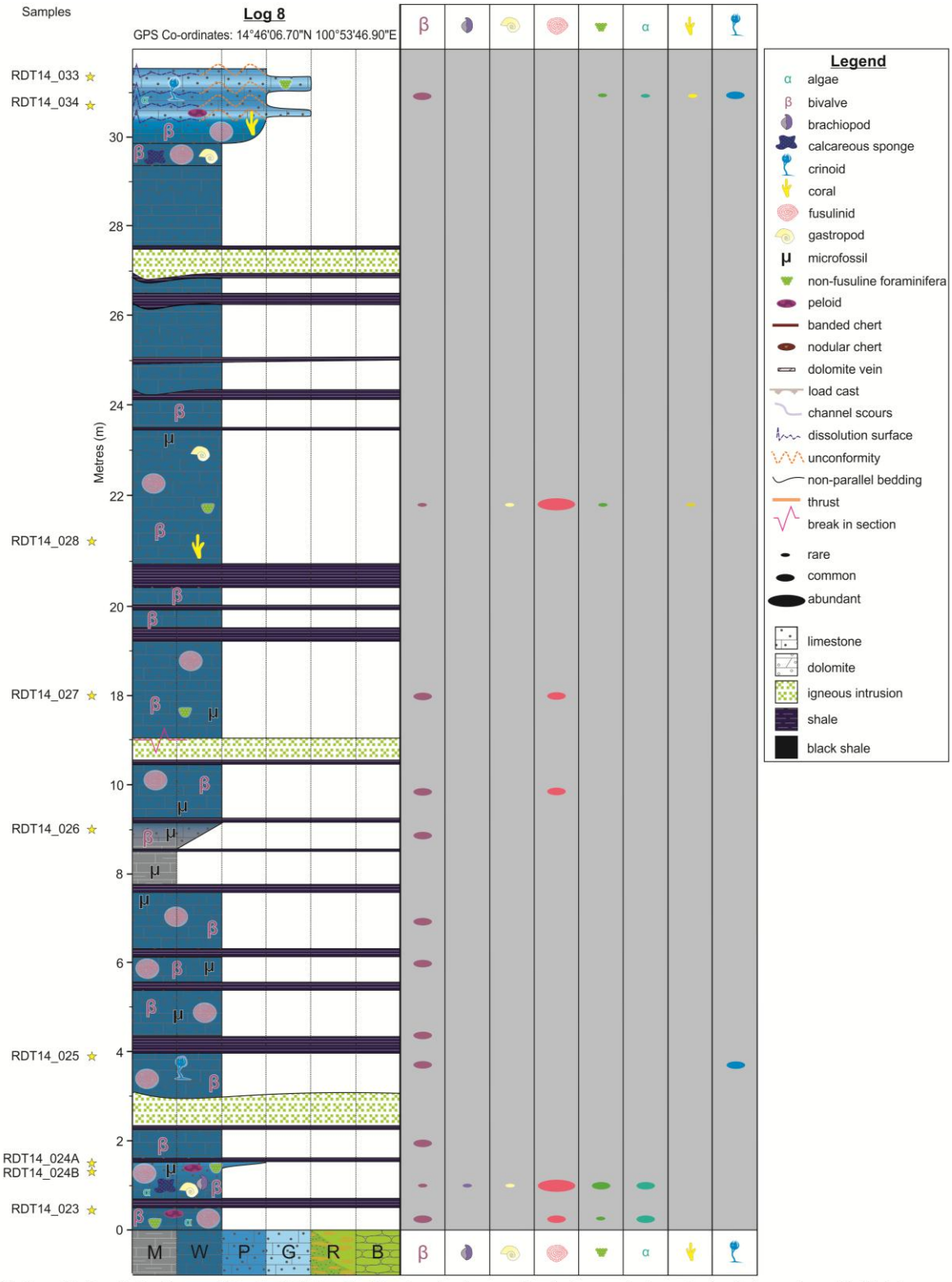

Stratigraphic Log 8: the Quarry of the North Below the Thrust region incorporating both macrofacies and microfacies analyses. M=Mudstone, W=Wackestone, P=Packstone, G=Grainstone, R=Rudstone, B=Boundstone

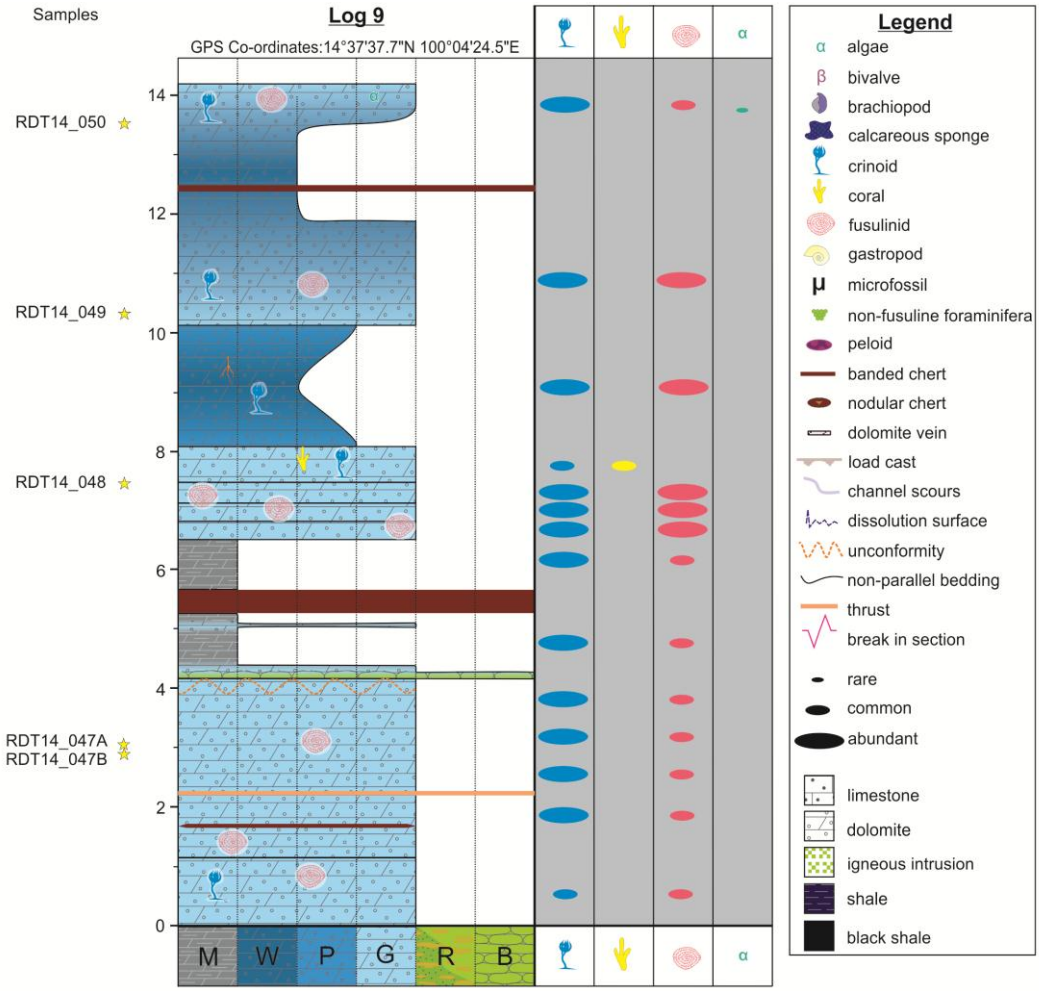

Stratigraphic Log 9: the Siam City Cement Alum Shale region incorporating both macrofacies and microfacies analyses. M=Mudstone, W=Wackestone, P=Packstone, G=Grainstone, R=Rudstone, B=Boundstone

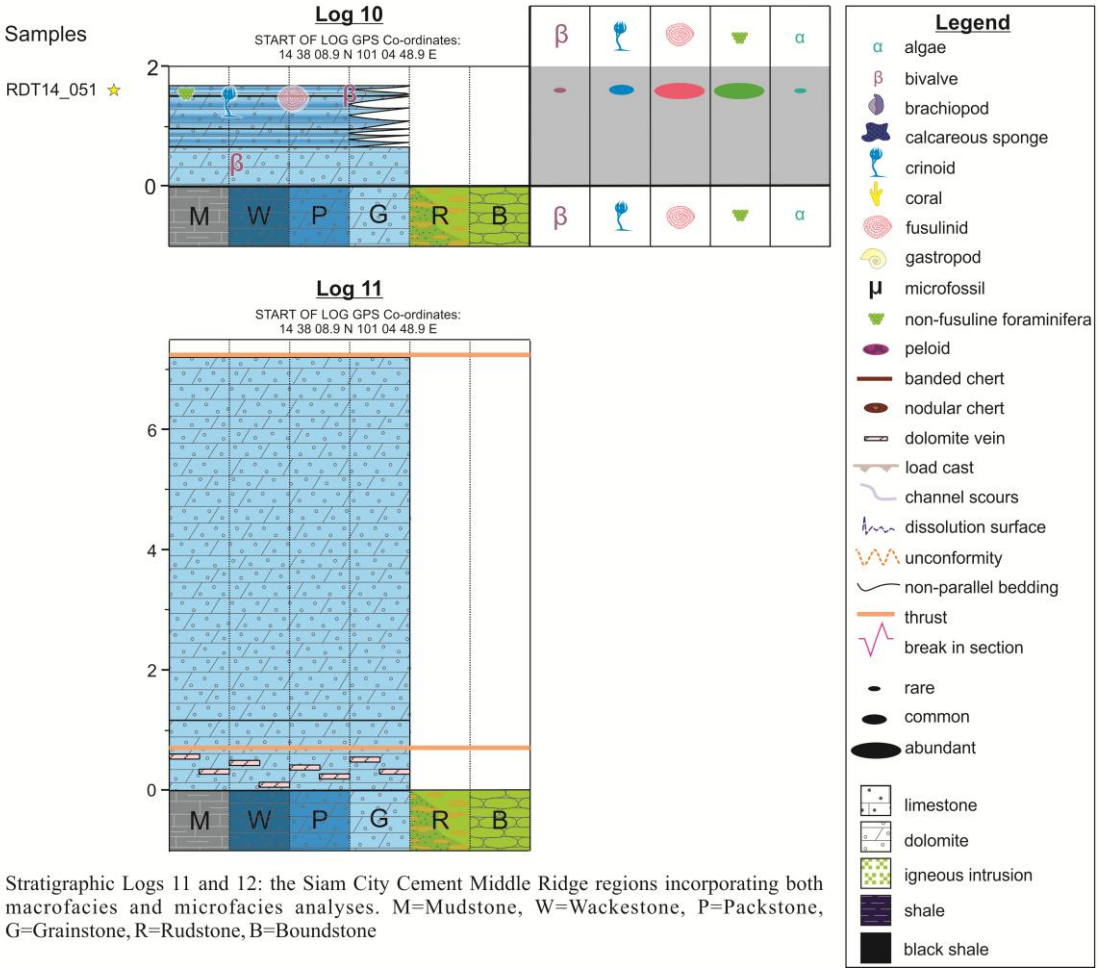

Stratigraphic Logs 11 and 12: the Siam City Cement Middle Ridge regions incorporating both macrofacies and microfacies analyses. M=Mudstone, W=Wackestone, P=Packstone, G=Grainstone, R=Rudstone, B=Boundstone

APPENDIX C: CORAL STRUCTURAL ELEMENTS

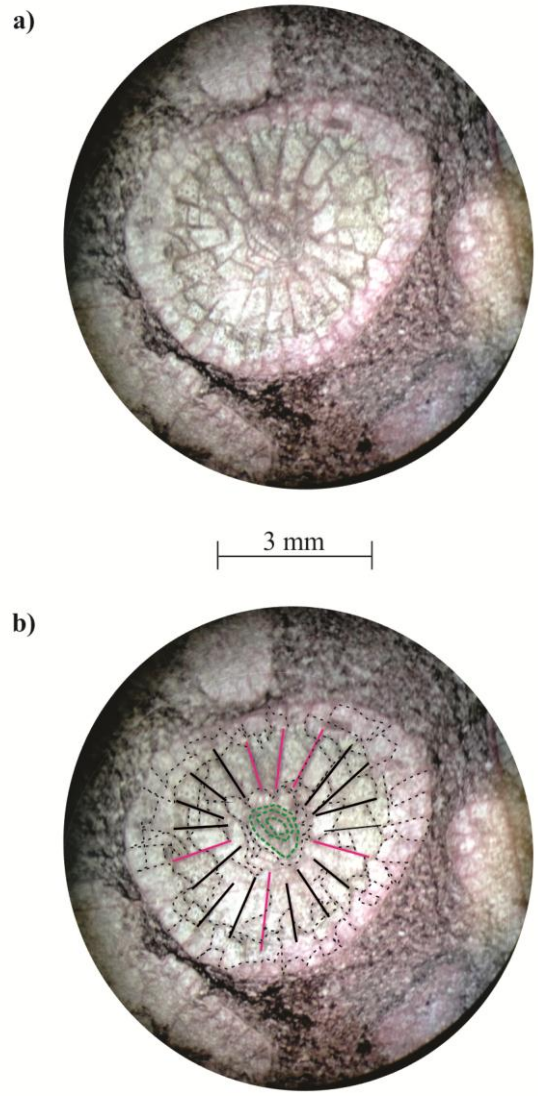

a) RDT14_005 thin section of a Permian rugose coral, part of a dendroid colony, a *Waagenophyllum* sp. stained with Alizarin Red and potassium ferricyanide under plain polarised light b) Highlighted coral structural elements: acrocolumella axial column in green, rectiform septal type as dashed lines and septal groups of major protosepta in pink and minor metasepta in black. Information determined using Easton (1944), Fontaine et al. (1988) and Dawson & Racey (1993).

REFERENCES

AYAN T. 1965. Chemical staining methods used in the identification of carbonate minerals, *Bulletin of the Mineral Research and Exploration Institute of Turkey*, 133-147.

BELLIER J.-P., MATHIEU R. & GRANIER B. 2010. Short Treatise on Foraminiferology.

BOUDAGHER-FADEL M. K. 2008a The Palaeozoic larger benthic foraminifera: the Carboniferous and Permian. In BOUDAGHER-FADEL M. K. ed. Developments in Palaeontology and Stratigraphy. pp. 39-118. Elsevier.

--- 2008b Biology and evolutionary history of larger benthic foraminifera. In BOUDAGHER-FADEL M. K. ed. Developments in Palaeontology and Stratigraphy. pp. 1-37. Elsevier.

DAWSON O. & RACEY A. 1993. Fusuline-calcareous algal biofacies of the Permian Ratburi Limestone, Saraburi, Central Thailand, *Journal of Southeast Asian Earth Sciences* **8**, 49-65.

DICKSON J. A. D. 1966. Carbonate identification and genesis as revealed by staining, *Journal of Sedimentary Petrology* **36**, 491-505.

FLÜGEL E. 2010 Microfacies of Carbonates Rocks. Springer, London.

HAYNES J. R. 2001 Foraminifera. eLS. John Wiley & Sons, Ltd.

KENDALL C. G. S. C. & FLOOD P. 2011 Classification of Carbonates. Encyclopedia of Modern Coral Reefs. pp. 193-198. Netherlands: Springer.

LOEBLICH A. R. & TAPPAN H. 1987 Foraminiferal genera and their classification. Van Nostrand Reinhold, New York.

SARTORIO D. & VENTURINI S. 1988 Southern Tethys Biofacies. Azienda Generale Italiana Petroli (AGIP), Italy.

SCHOLLE P. A. & ULMER-SCHOLLE D. S. 2003 A Color Guide to the Petrography of Carbonate Rocks: Grains, Textures, Porosity, Diagenesis, AAPG Memoir 77. American Association of Petroleum Geologists, Tulsa.

THAMBUNYA S., PISUTHA-ARNOND V. & KHANTAPRAB C. 2007. Depositional Environments of Permian Rocks of the Khao Khad Formation in Central Thailand, *ScienceAsia* **33**, 371-381.

TUCKER M. E. 2001 Limestones. Sedimentary petrology: an introduction to the origin of sedimentary rocks. pp. 110-165. United Kingdom: Blackwell Publishing, 3 ed.